

**Investigation of Effects of Moisture Susceptibility of Warm Mix  
Asphalt (WMA) Mixes on Dynamic Modulus and Field Performance**

by

Yichao Xu

A Thesis

Submitted to the Faculty

of the

WORCESTER POLYTECHNIC INSTITUTE

in partial fulfillment of the requirements for the

Degree of Master of Science

in

Civil Engineering

---

December 2011

Approved

---

Professor Rajib B. Mallick, Major Advisor, CEE

---

Professor Mingjiang Tao, Co-advisor, CEE

---

Professor Tahar El-Korchi, Department Head, CE

## **Abstract**

Residual moisture from incompletely dried aggregates would most likely remain in the Warm Mix Asphalt (WMA) due to its lower production and compaction temperature, resulting in harmful effects on field performance. Dynamic modulus has been recognized as a parameter that reflects the overall behavior of asphalt mixtures and possesses promising correlations with field performance. This study aims to investigate the effects of moisture susceptibility of WMA on dynamic modulus and simulate the field performance with the aid of Mechanistic-Empirical Pavement Design Guide (MEPDG) software. Four distinct sets of WMA specimens were prepared as follows: 1. fully dried aggregates without moisture conditioning; 2. fully dried aggregates with moisture conditioning; 3. incompletely dried aggregates without moisture conditioning; and 4. incompletely dried aggregates with moisture conditioning. Simple Performance Test (SPT) was employed to collect the raw data of dynamic modulus tests and master curves were constructed from the reduced data using Hirsch model. The results show that moisture can negatively influence the dynamic modulus values and moisture conditioning had more effect than residual moisture from incompletely dried aggregates. Two types of distress, fatigue cracking and rutting, were analyzed in the simulation. Moisture can significantly decrease the resistance against rutting and to a lesser extent, the resistance against fatigue cracking.

## **Acknowledgements**

I would like to extend much appreciation and gratitude to my advisor Dr. Rajib B. Mallick and co-advisor Dr. Mingjiang Tao for all their help and guidance. Particularly, when Dr. Mallick was taking sabbatical leave in India, Dr. Tao gave me more precious advice during tests and thesis writing. I also would like to thank Dr. Tahar El-Korchi, head of the department, for providing his valuable advice about the thesis. Without their help and encouragement of my thesis committee, this study would not have been possible.

I would like to thank Don Pellegrino, lab manager of CEE department, Russ Lang, lab assistant and the following students: Rudy Pinkham, Ryan Worsman, Hong Guo, Liwen Fei and Wenyi Gong for their unselfish help in either testing or data analysis.

Finally, I would like to acknowledge the help of Maine Department of Transportation for providing the research materials.

# Table of Contents

Abstract.....	i
Acknowledgements.....	ii
List of Figures.....	iv
List of Tables.....	v
1. Introduction.....	1
1.1 Background.....	1
1.2 Objective.....	2
2. Literature Review.....	3
2.1 Warm Mix Asphalt (WMA).....	3
2.1.1 Overview and Prospect.....	3
2.1.2 Moisture Susceptibility of WMA.....	4
2.2 Dynamic Modulus.....	5
2.2.1 Basic Conception and Testing Method.....	5
2.2.2 Establishment and Method Selection of Master Curve.....	6
2.3 Mechanistic-Empirical Pavement Design Guide (MEPDG).....	10
3. Methodology.....	12
3.1 Material Selection.....	12
3.2 Experimental Design.....	13
3.3 Dynamic Modulus Test.....	18
4. Results and Analysis.....	22
4.1 Control of Moisture to Achieve Incomplete Drying.....	22
4.2 Volumetric Properties.....	25
4.3 Dynamic Modulus Test and Master Curve.....	26
4.3.1 Dynamic Modulus and Phase Angle Results.....	26
4.3.2 ANOVA for Dynamic Modulus Results.....	32
4.3.3 Development of Master Curve.....	35
4.4 MEPDG Analysis.....	40
4.4.1 Inputs and Analysis.....	40
4.4.2 Results of Analysis.....	42
5. Conclusions.....	46
6. Recommendations.....	47
References.....	48
Appendix A: Control of Incomplete Dry.....	50
Appendix B: Volumetric Properties.....	52
Appendix C: Dynamic Modulus Test and Master Curve.....	58
Appendix D: ANOVA for Dynamic Modulus Results.....	66
Appendix E: MatLAB Code for $G^*$ Back Calculation.....	69
Appendix F: MatLAB Code for Reduction of Dynamic Modulus Results.....	70

## List of Figures

Figure 1. Advantages of Warm Mix Asphalt.....	4
Figure 2. General Flow Chart for Experimental Design.....	14
Figure 3. Warm Mixing and Compaction Process .....	16
Figure 4. Coring and Cutting Process .....	17
Figure 5. Freeze-thaw Cycle .....	18
Figure 6. Dynamic Modulus Test.....	19
Figure 7. Specimen Test Results of Dynamic Modulus Test .....	19
Figure 8. Moisture Contents of Set 3.....	23
Figure 9. Moisture Contents (Last 2 Hours) of Set 3.....	23
Figure 10. Moisture Contents of Set 4.....	24
Figure 11. Moisture Contents (Last 2 Hours) of Set 4.....	24
Figure 12. Void in Total Mix (VTM) for Dynamic Modulus Tests.....	25
Figure 13. Dynamic Modulus Results at 4.4°C .....	27
Figure 14. Dynamic Modulus Results at 21.1°C .....	27
Figure 15. Dynamic Modulus Results at 37.8°C .....	28
Figure 16. Dynamic Modulus Results at 54.4°C .....	28
Figure 17. Phase Angle Results at 4.4°C .....	29
Figure 18. Phase Angle Results at 21.1°C .....	29
Figure 19. Phase Angle Results at 37.8°C .....	30
Figure 20. Phase Angle Results at 54.4°C .....	30
Figure 21. $ E^* /\sin\delta$ Results for 54.4°C.....	31
Figure 22. $ E^* \sin\delta$ Results for 21.1°C.....	32
Figure 23. ANOVA Analysis at 4.4°C.....	33
Figure 24. ANOVA Analysis at 21.1°C.....	34
Figure 25. ANOVA Analysis at 37.8°C.....	34
Figure 26. Predicted $E^*$ vs. Measured $E^*$ of Set 1 .....	37
Figure 27. Predicted $E^*$ vs. Measured $E^*$ of Set 2 .....	37
Figure 28. Predicted $E^*$ vs. Measured $E^*$ of Set 3 .....	38
Figure 29. Predicted $E^*$ vs. Measured $E^*$ of Set 4 .....	38
Figure 30. Dynamic Modulus Master Curve of Four-set Mixtures.....	39
Figure 31. Propagation Trend of the Alligator Cracking .....	43
Figure 32. Propagation Trend of Rutting of Asphalt Concrete Layer.....	45
Figure 33. Propagation Trend of Rutting of Entire Pavement .....	45

## List of Tables

Table 1. Recommended Equilibrium Times.....	7
Table 2. Mixture Gradation and Water Absorption of Herman Aggregates .....	12
Table 3. Mass of Loose Mix for One Gyratory Specimen .....	15
Table 4. Temperature Equilibrium Time for $E^*$ Test .....	20
Table 5. Dynamic Modulus Testing Loads .....	20
Table 6. The Meaning of Variance Numbers .....	35
Table 7. Back Calculating $G^*$ at 10 Hz.....	41
Table 8. Properties of Asphalt Pavement Layers .....	41
Table 9. Predicted Alligator Cracking and Years to Failure.....	42
Table 10. Rutting Depth of the Asphalt Concrete Layer and Years to Failure.....	43
Table 11. Rutting Depth of the Entire Pavement and Years to Failure .....	43
Table 12. The Change of the Aggregate Mass and Moisture Contents of Set 3 .....	50
Table 13. The Change of the Aggregate Mass and Moisture Contents of Set 4 .....	51
Table 14. The Data Analysis of Theoretical Maximum Specific Gravity ( $G_{mm}$ ).....	52
Table 15. The Data Analysis of Bulk Specific Gravity and Air Voids of Set 1.....	53
Table 16. The Data Analysis of Bulk Specific Gravity and Air Voids of Set 2.....	54
Table 17. The Data Analysis of Bulk Specific Gravity and Air Voids of Set 3.....	55
Table 18. The Data Analysis of Bulk Specific Gravity and Air Voids of Set 4.....	56
Table 19. The Average and Standard Deviation of VTM.....	57
Table 20. The Average of Dynamic Modulus and Phase Angle Results .....	58
Table 21. $ E^* /\sin\delta$ and $ E^* *\sin\delta$ Results .....	59
Table 22. Std./Ave. of $E^*$ Results of Set 1 .....	60
Table 23. Std./Ave. of $E^*$ Results of Set 2.....	60
Table 24. Std./Ave. of $E^*$ Results of Set 3.....	61
Table 25. Std./Ave. of $E^*$ Results of Set 4.....	61
Table 26. Computational Process of Master Curve of Set 1 .....	62
Table 27. Computational Process of Master Curve of Set 2 .....	63
Table 28. Computational Process of Master Curve of Set 3 .....	64
Table 29. Computational Process of Master Curve of Set 4 .....	65
Table 30. SNK Analysis of Homogeneous Subsets at 4.4°C .....	66
Table 31. SNK Analysis of Homogeneous Subsets at 21.1°C .....	67
Table 32. SNK Analysis of Homogeneous Subsets at 21.1°C .....	68

# 1. Introduction

## 1.1 Background

Warm Mix Asphalt (WMA), as a newly developing technology for constructing asphalt pavement, is being widely adopted by many State Departments of Transportation (DOTs). From the advent of this new technology to more than ten years' development, a significant amount of laboratory research associated with field performance has found and further verified that even though WMA possesses several evident advantages compared with traditional Hot Mix Asphalt (HMA), including lower temperatures of producing, placing and compacting (lower by 30-100°F) resulting in less fuel consumption as well as the emissions of greenhouse gases, a concern of moisture susceptibility has to be investigated to predict the long term performance [1-3]. Since WMA construction follows the existing HMA Superpave standards and procedures [1], temperature becomes the key point which differentiates these two technologies. During the production of WMA, aggregates cannot be heated up to as high a temperature as is used for HMA; in another case water is required to be added into the mixture to reduce the viscosity of asphalt binder. Therefore, under certain circumstances some residual moisture would probably remain trapped inside the mix, and this could inevitably cause an exacerbation of loss of adhesion between the asphalt binder and the aggregates, leading to moisture induced damage and premature failure of pavements [3].

To evaluate the influence of moisture susceptibility of WMA mixes on their mechanical properties, W. Gong [4] has conducted three mechanical tests from various asphalt mixes, including resilient modulus ( $M_r$ ), creep compliance and indirect tensile test (IDT). Based on the results of these tests, fracture mechanics energy ratios calculated from completely and incompletely dried WMA samples with and without moisture conditioning process demonstrated that the moisture has an appreciable impact on the overall behavior of asphalt mixes. Dynamic modulus,  $E^*$ , is another essential mechanical property which has been recognized to reflect the overall behavior of asphalt mixtures and possess promising correlations with field performance [5]. Dynamic modulus master curves are constructed after a series of data reduction and numerical optimization to distinguish between good and poor mixture properties over a wide range of temperatures and loading rates. The National Cooperative Highway Research Program (NCHRP) Report 589 [6] recommended the use of the dynamic modulus test for moisture susceptibility evaluation and Report 614 [7] elaborates on the specification for the Simple Performance Test System (SPT) with Hirsch Model to conduct dynamic modulus test more practically and economically. Both reports indicate that the dynamic modulus is also a primary material

input for flexible pavement structural design and analysis in the Mechanistic-Empirical Pavement Design Guide (MEPDG) used for Long-Term Pavement Performance (LTPP) prediction, such as rutting and fatigue cracking. Until now MEPDG is still in the stage of exploration and development and there exist calibration issues during the use of MEPDG to predict pavement performance. However, most researchers agree that the MEPDG is an excellent tool for bridging moisture susceptibility of asphalt mixtures and distress levels of the associated pavements [8, 9].

## **1.2 Objective**

The objective of this research is to investigate the influences of moisture susceptibility of WMA mixes on dynamic modulus, which is used as the input for predicting field performance in MEPDG. Some specific objectives are listed below:

1. Procure reliable and acceptable data from dynamic modulus tests with completely and incompletely dried WMA specimens with and without moisture conditioning process;
2. Analyze and compare data and develop dynamic modulus master curves for various specimens so as to assess the effects of moisture susceptibility of WMA mixes on dynamic modulus;
3. Input dynamic modulus measurements of different mixtures as well as other pertinent parameters to predict field performance and judge the acceptability of a mixture to resist permanent deformation and fatigue cracking with the aid of MEPDG.



## **2. Literature Review**

### **2.1 Warm Mix Asphalt (WMA)**

#### **2.1.1 Overview and Prospect**

Under the stimulation of three factors, i.e. economy, environment and health, warm mix asphalt, which is identified as one of ways to improve traditional HMA technology, emerged in the late 1990's in Europe. Very soon after put into practice, WMA has gained lots of interests in industry and academia, and then was introduced into United States in 2002 [2]. Due to its significant performance benefits, this emerging and challenging technology has become very attractive to State DOTs, which have started adopting this technology and conducting a significant amount of research for developing appropriate specifications.

HMA is produced at temperatures approximately 30-100°F higher than temperatures used in the production of WMA. Typically high temperature during the production of HMA is essential to drive all of the moisture away from the aggregates and to reduce asphalt binder viscosity for good aggregates coating as well as ease of placement and compaction [10]. The premise of employing WMA technology is to guarantee that WMA pavement must possess similar workability, durability and performance characteristics as HMA using substantially reduced temperature [11]. The reasons of selecting lower production temperature, or the advantages claimed for WMA are presented in Figure 1.

As mentioned previously, the most notable advantage of WMA is that significantly reduced temperatures are applied in the production process. To solve the problem that asphalt binder will be too stiff to coat aggregates at lower temperatures, either additives such as waxes, in asphalt binder or foamed asphalt are used [11]. With the continuous development of WMA technology, a number of different WMA processes have been developed, which can be categorized into three groups: organic additive, foaming and chemical additive [12]. Among numerous approaches, Sasobit<sup>®</sup> has been popularized most extensively for WMA projects in the United States as a kind of organic additive. Produced from coal gasification and supplied in pellet form, Sasobit is considered as “asphalt flow improver” on account of its ability to dramatically reduce asphalt viscosity at lower production temperature [1, 10, 11]. Typically, asphalt binder, like PG 64-28, with 1.5% Sasobit by weight of binder at 125°C has the similar viscosity as the unmodified binder at 150°C. However, it should be noted that there is no evidence of

improvement of binder performance, such as with respect to resistance against moisture damage, by adding Sasobit [13]. S.W. Goh & Yu Liu also found that the additional Sasobit can increase the value of dynamic shear modulus ( $G^*$ ) of asphalt binder significantly, resulting in the improvement of rutting resistance while reducing the resistance against fatigue cracking [14].

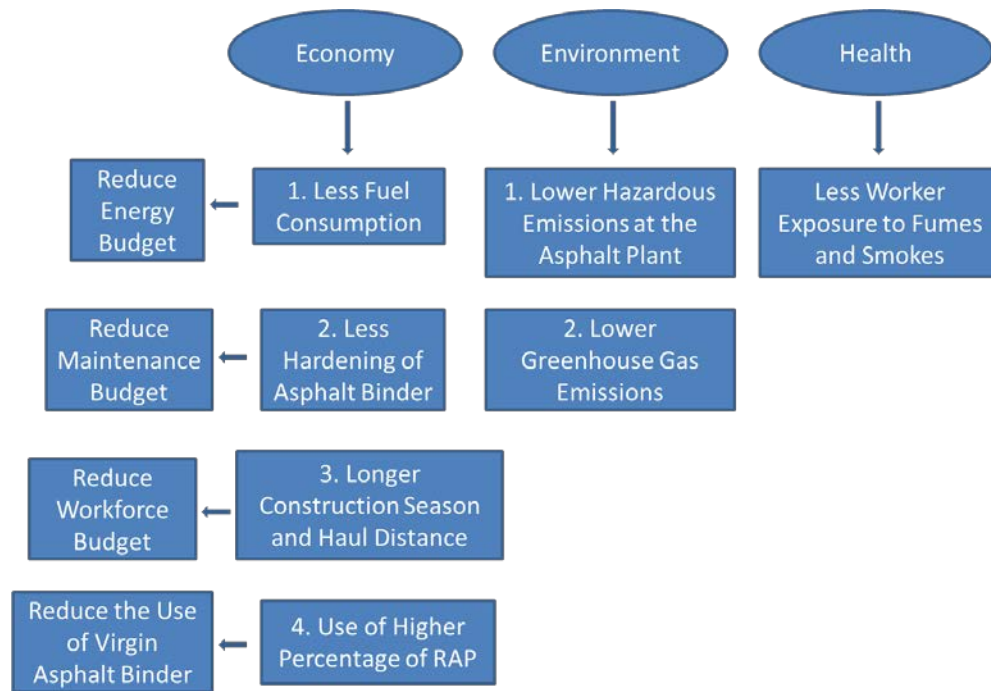


**Figure 1. Advantages of Warm Mix Asphalt**

Overall, increasingly stringent regulations regarding greenhouse gas emissions are making the necessity of reducing HMA production temperatures more intense, from which the economization of natural resources would also become possible [15]. So far, the development of WMA technology is not as mature and perfect as that of HMA, hence there needs to be more comprehensive research to compensate for the lack of laboratory and field data with respect to performance, durability and compatibility of WMA.

### 2.1.2 Moisture Susceptibility of WMA

The most major concern for WMA is the potential moisture susceptibility of the pavement since significantly reduced production and compaction temperatures might lead to incomplete drying of aggregates, and therefore presence of residual moisture, which could have negative influence on pavement performance, such as rutting, stripping and

fatigue cracking. On one hand, given the limited drying time and relatively low temperatures, aggregates may not dried sufficiently, leading to certain amount of moisture trapped in the mixture; on the other hand, to reduce binder viscosity, additives or foaming technologies may be introduced into asphalt binder. Furthermore, these pavements could be subjected to moisture during rainy seasons. Any moisture remaining in or on the aggregates would affect aggregate coating and exacerbate the loss of bond between asphalt binder and aggregates, causing asphalt stripping and premature pavement failure. Typically the loss of bond begins at the bottom of the pavement layer and progresses upward [10].

## 2.2 Dynamic Modulus

### 2.2.1 Basic Conception and Testing Method

Dynamic modulus, normally identified as  $|E^*|$ , is an absolute value of the complex modulus  $E^*$ , defined the stress-strain relationship of linear viscoelastic materials subjected to continuously applied sinusoidal loading within a specified frequency range. In terms of mathematics, dynamic modulus is the ratio of the amplitude of the sinusoidal stress ( $\sigma_0$ ) at any given time and angular load frequency to the amplitude of the recoverable axial strain ( $\varepsilon_0$ ) at the same time and frequency [16, 17]. The basic expression of dynamic modulus is shown as Equation 1.

$$|E^*| = \frac{\sigma_0}{\varepsilon_0} \quad (1)$$

Another primary parameter that is determined from the dynamic modulus test is phase angle ( $\phi$ ), defined as the angle by which  $\varepsilon_0$  lags behind  $\sigma_0$  [17]. It is a direct indicator of the viscoelastic property of HMA. For materials with viscoelastic characteristic, the range of the phase angle is always between  $0^\circ$  and  $90^\circ$ , which means the phase difference between  $\sigma_0$  and  $\varepsilon_0$  stays within one quarter of a sinusoidal cycle. For those two extreme points,  $\phi=0^\circ$  corresponds to a purely elastic material and  $\phi=90^\circ$  corresponds to a purely viscous material. Besides dynamic modulus can reflect the quality of mixtures,  $|E^*|/\sin\delta$  measured at high temperature is regarded as a good indicator of rutting susceptibility and  $|E^*|\sin\delta$  acquired at intermediate temperature is recommended to evaluate the fatigue resistance of asphalt mixtures [18, 19].

The development of dynamic modulus test has experienced an improvement process, which enables laboratory researchers and highway agencies to conduct tests with shorter

overall time and a reasonable cost for establishing precise results. Dynamic modulus test specimens should be manufactured by coring and cutting cylindrical specimens 100-104 mm (3.94-4.09 in.) in diameter and 147.5-152.5 mm (5.81-6.00 in.) in height from the middle of gyratory compacted specimens that are 150 mm (5.90 in.) in diameter and 165-175 mm (6.50-6.90 in.) in height [6, 7, 17]. A Superpave Gyratory Compactor is used for compaction and the resulting test specimen should be cylindrical with sides that are smooth, parallel, and free from steps, ridges and grooves [17]. Referred to NCHRP Report 589, there are three reasons for coring out smaller specimen: 1. to obtain an appropriate height-to-diameter ratio for the test specimens, the minimum of which is 1.5; 2. to eliminate areas of high air voids in the gyratory specimens, which refers to the ends and the circumference; and 3. to obtain relatively smooth, parallel ends for testing [6].

AASHTO TP 62-03, “*Standard Method of Test for Determining Dynamic Modulus of Hot-Mix Asphalt Concrete Mixtures*”, recommends a standard procedure for running dynamic modulus test, which consists of testing a minimum of two replicate specimens at temperatures of -10, 4.4, 21.1, 37.8, and 54.4°C (14, 40, 70, 100, and 130°F) at loading frequencies of 25, 10, 5, 1.0, 0.5, and 0.1 Hz at each temperature [20]. Prior to conducting tests, the mounting of studs for the axial Linear Variable Differential Transformer (LVDT) are required to the sides of the specimen using mounting frames and quick setting epoxy. The function of LVDT is to measure the deformations of the specimen when it is subjected to a continuous sinusoidal loading at a certain temperature and frequency. Three LVDTs located 120° apart are recommended for more accurate testing results and for minimizing the number of replicate specimen required for testing, but two LVDTs on opposite sides of the specimen are also acceptable.

### **2.2.2 Establishment and Method Selection of Master Curve**

Using the principle of time-temperature superposition, dynamic modulus master curves are constructed through a series of data reduction and numerical optimization. Basically, a standard reference temperature, i.e. 70°F is selected, and then data at various temperatures are shifted with respect to loading frequency until the curves merge into a single smooth function [7]. The master curve of modulus has two forms to illustrate the property of materials, the frequency or time (the reciprocal of the frequency) dependency and the temperature dependency. Therefore, to comprehensively describe the rate and temperature effects, both the master curve and the shift factors are necessary.

As mentioned in the last part, a database of 60 dynamic modulus measurements obtained from two replicate specimens subjected to five temperatures with six different frequencies are needed for determining the parameters of the master curve by numerical optimization. Based on the considerations of economy and environment as well as

shortening the overall test-conducting time, this standard method of establishing the dynamic modulus master curve needs to be improved and abbreviated. It would take a significant amount of time to measure 60 values since specimens inside the environmental chamber need at least two hours to change temperatures. According to Table 1, minimum equilibrium temperature times are listed on the basis of the most of laboratory testing data [17]. Also, on the low temperature testing requirement at 14°F significantly increases the cost of the environmental system and necessitates an increase in the loading capacity of the testing equipment; there is also the difficulty of controlling moisture condensation and ice formation, and potential damage of the loading machine, resulting from more rigid specimens [7].

**Table 1. Recommended Equilibrium Times**

<b>Specimen Temperature, °C (°F)</b>	<b>Time from Room Temperature 25°C (77°F), hrs</b>	<b>Time from Previous Test Temperature, hrs</b>
-10 (14)	Overnight	-
4.4 (40)	Overnight	4hrs or overnight
21.1 (70)	1	3
37.8 (100)	2	2
54.4 (130)	2	1

NCHRP 9-29 [7] describes an approach of using Simple Performance Test (SPT) to develop the dynamic modulus master curve for asphalt concrete mixtures. This approach, employs the Hirsch model to estimate the limiting maximum modulus of the mixture based on volumetric properties and a limiting binder shear modulus of 1 GPa (145,000 psi); it is very similar to the method described in AASHTO TP 62-03, except that a reduced number of temperatures of 4.4, 21.1, and 46.1°C (40, 70, and 115°F), an expanded range of frequencies of 10, 1.0, 0.1, and 0.01 Hz as well as an estimate of the limiting maximum modulus are utilized. There are only 24 measurements needed, and the testing temperature below zero Celsius is eliminated.

Equation 2 is the final form of  $E^*$  that is used in the MEPDG for the development of master curves from laboratory test data.

$$\log(E^*) = \delta + \frac{\alpha}{1 + e^{\beta + \gamma \{ \log(t) - c [10^{A+VTS \cdot \log T} - 10^{A+VTS \cdot \log(529.67)}] \}}} \quad (2)$$

where:

$E^*$  = dynamic modulus

$t$  = loading time

$T$  = temperature, Rankine

$A, VTS$  = viscosity-temperature relationship parameters for RTFOT aging

- $c$  = fitting parameter
- $\delta$  = minimum value of  $E^*$
- $\delta + \alpha$  = maximum value of  $E^*$
- $\beta, \gamma$  = parameters describing the shape of the sigmoidal function

The fitting parameters ( $\alpha, \beta, \delta, \gamma$ , and  $c$ ) are determined through numerical optimization using mixture test data collected in accordance with AASHTO TP 62-03.

Another form of equation for constructing the master curve without the viscosity-temperature relationship can be given as Equation 3.

$$\log(E^*) = \delta + \frac{\alpha}{1 + e^{\beta + \gamma \left\{ \log(t) - \frac{\Delta E_a}{19.14714} \left[ \left( \frac{1}{T} \right) - \left( \frac{1}{295.25} \right) \right] \right\}}} \quad (3)$$

where:

- $E^*$  = dynamic modulus
- $t$  = loading time
- $T$  = temperature, K
- $\Delta E_a$  = activation energy, J/mol
- $\delta$  = minimum value of  $E^*$
- $\delta + \alpha$  = maximum value of  $E^*$
- $\beta, \gamma$  = parameters describing the shape of the sigmoidal function

The fitting parameters ( $\alpha, \beta, \delta, \gamma$ , and  $c$ ) are determined through numerical optimization in the same way.

In accordance with AASHTO TP 62-03, test data from a wide range of temperatures including the low temperature below zero are developed to properly fit the master curves in Equation 2 and 3 [20]. As demonstrated before, low temperature is a disadvantage for conducting dynamic modulus tests because of higher cost on humidity control and greater loading levels. NCHRP 9-29 presents an improved equation, which is determined over a narrow range of temperatures with respect to SPT, by introducing the Hirsch model. Equation 4 and 5 explain the Hirsch model, which allows the estimation of the modulus of the mixture from binder stiffness data and volumetric properties [7].

$$|E^*|_{mix} = P_c \left[ 4,200,000 \left( 1 - \frac{VMA}{100} \right) + 3|G^*|_{binder} \left( \frac{VFA \times VMA}{10,000} \right) \right] + \frac{1 - P_c}{\left[ \frac{\left( 1 - \frac{VMA}{100} \right)}{4,200,000} + \frac{VMA}{3VFA|G^*|_{binder}} \right]} \quad (4)$$

where:

$$P_c = \frac{\left( 20 + \frac{VFA \times 3|G^*|_{binder}}{VMA} \right)^{0.58}}{650 + \left( \frac{VFA \times 3|G^*|_{binder}}{VMA} \right)^{0.58}} \quad (5)$$

$VMA$  = Voids in mineral aggregates, %  
 $VFA$  = Voids filled with asphalt, %  
 $|G^*|_{\text{binder}}$  = shear complex modulus of binder, psi

Substitution of the estimate of the maximum shear modulus for all binder, which is approximately 1 GPa or 145,000 psi, into Equation 4 and 5 yields the limiting maximum modulus ( $|E^*|_{\text{max}}$ ) of asphalt concrete mixtures from volumetric data.

On the premise that the limiting maximum modulus has been calculated, MEPDG master curve relationship given in Equation 2 and 3 can be presented as follows without the parameter  $\alpha$ :

$$\log(E^*) = \delta + \frac{(Max - \delta)}{1 + e^{\beta + \gamma \{ \log(t) - c [10^{A+VTS \cdot \log T} - 10^{A+VTS \cdot \log(529.67)}] \}}} \quad (6)$$

where:

$E^*$  = dynamic modulus  
 $t$  = loading time  
 $T$  = temperature, Rankine  
 $A, VTS$  = viscosity-temperature relationship parameters for RTFOT aging  
 $Max$  = limiting maximum modulus  
 $\beta, \delta, \gamma$  and  $c$  = fitting parameters

and

$$\log(E^*) = \delta + \frac{(Max - \delta)}{1 + e^{\beta + \gamma \{ \log(t) - \frac{\Delta E_a}{19.14714} \left[ \left( \frac{1}{T} \right) - \left( \frac{1}{295.25} \right) \right] \}}} \quad (7)$$

where:

$E^*$  = dynamic modulus  
 $t$  = loading time  
 $T$  = temperature, K  
 $Max$  = limiting maximum modulus  
 $\beta, \delta, \gamma$  and  $\Delta E_a$  = fitting parameters

With the aid of the Solver function in Microsoft EXCEL<sup>®</sup>, all the fitting parameters can be obtained through numerical optimization using the measured data and abbreviated master curve relationship, and shift factor can finally be determined. Briefly, this is done by setting up a spreadsheet, plugging in all the parameters and data which would be employed for optimization and computing the sum of the squared errors between the logarithm of the measured dynamic moduli and the values predicted by abbreviated equations. The last step is utilizing Solver function to minimize the sum of the squared errors by varying the fitting parameters.

## **2.3 Mechanistic-Empirical Pavement Design Guide (MEPDG)**

Mechanistic-Empirical Pavement Design Guide (MEPDG) is a new design guide published in 2002 for rigid and flexible pavement design with the purpose of improving all the preceding design guides with proper consideration of currently existing paving materials and technologies, the different climatic zones in the US, as well as the continuously increased traffic volumes [21]. Before the advent of MEPDG, American Association of State Highway and Transportation Officials (AASHTO) Design Guide, based on the results of its road tests in 1958, was the predominant specification used to design pavements by most State DOTs [9]. But this empirical guide had a significant amount of limitations such as the use of 1950's materials, traffic volumes and construction methods as well as simple considerations of climate and pavement layers, and the use of serviceability concept rather than any mechanistic criteria. These perceptible deficiencies motivated AASHTO to pursue a more reliable design, leading to the emergence of MEPDG, which was developed under National Cooperative Highway Research Program (NCHRP) Project 1-37A. The guide summarized former pavement design procedures and also combined some valuable empirical experience with newly-developed mechanistic models, from which stresses, strains and deformations in the pavement were used in conjunction with transfer functions to predict its performance. The other most significant feature presented in this guide is the incorporation of the impact of climate of more than 800 areas and detailed traffic conditions in the form of biweekly and monthly iterative predictions for the entire design life of the pavement [9]. The predictions of the development and propagation of primary pavement distress, including rutting and fatigue cracking can also be comprehensively calibrated by selected mechanistic-based distress prediction models.

MEPDG is not only a comprehensive pavement design guide, but also a powerful and user-friendly software package that is based on the principle of the design guide. One of the notable characteristics of this software is the selection of design levels since MEPDG provides three hierarchical levels, namely Level 1, Level 2 and Level 3, which rank from highest to the lowest level of accuracy, trafficked pavements as well as safety and economic considerations. It is obvious that more specific is the data, higher is the accuracy with which the results could be predicted. For example, only test data or site-specific information can be used as inputs in Level 1; otherwise, lower levels will be selected for using general and historical data [22]. Since each model has its unique sensitivity to certain inputs which would affect the prediction accuracy, it is crucial to investigate the most useful inputs and the appropriate level that determine the accuracy of models. A mix of levels might be used to accommodate different accuracy of inputs



plugged into this software, such as asphalt mix properties specified in Level 1, traffic data in Level 2 and subgrade properties assigned in Level 3. With the aim of easily plugging inputs into software and conveniently classifying large amounts of data, three major categories, including traffic, climate and material, are offered for designing or analyzing a pavement. The guide is also integrated with a climate database and Enhanced Climatic Integrated Model (ECIM), which is used to model temperature and moisture within each pavement layer including the subgrade.

With regard to this project, MEPDG is not employed for designing a new pavement, but was used for the field performance and predicting possible distress on the basis of dynamic modulus. As demonstrated earlier, dynamic modulus is a reliable parameter which can reflect the overall behavior of asphalt pavement and has a close relationship with field performance. Specifically, as the first-hand test data, dynamic modulus values can be used in Level 1 of asphalt material properties. Therefore, in order to acquire more precise predicted results, dynamic modulus measurements are indispensable inputs when using this software to simulate pavement performance.

### 3. Methodology

#### 3.1 Material Selection

##### *Aggregate*

All the aggregates used in this research were provided by Maine DOT. There were a total of five different aggregate sizes, including 12.5 mm stone, 9.5 mm stone, minus 9.5 mm stone, sand and washed ledge sand. According to the specification of Maine DOT, these five kinds of aggregates were blended to meet the job mix formula gradation. The bulk specific gravity of the blend was 2.66 and the water absorption was 1.8%. The mixture gradation and the water absorption values are shown in Table 2.

**Table 2. Mixture Gradation and Water Absorption of Herman Aggregates**

<b>Sieve Size (mm)</b>	<b>Percent of Passing</b>	<b>Job Mix Formula</b>
1/2 (12.5)	100	100
3/8 (9.5)	93.2	90-100
4 (4.75)	70.1	68-90
8 (2.36)	41.0	32-67
16 (1.18)	32.1	-
30(0.6)	18.7	-
50 (0.3)	12.9	-
100 (0.15)	7.3	-
200 (0.075)	2.4	2-10
<b>Water Absorption</b>	1.8% (combined blend of coarse and fine aggregates)	

##### *Asphalt*

The virgin asphalt binder utilized in this research was a PG 64-28 grade binder also provided by Maine DOT.

##### *WMA Additive*

For the sake of coating aggregate completely at warm temperature, Sasobit as the WMA additive was selected to ensure low viscosity of the asphalt binder. Sasobit was pre-mixed with liquid asphalt binder at 125°C at the dosage of 1.5% by weight of total asphalt binder and then this modified asphalt was stored for subsequent process.

## 3.2 Experimental Design

With the purpose of fully investigating the influences of moisture susceptibility of WMA mixes on dynamic modulus and simulating situations occurring in field, four sets of samples were tested: **Set 1** prepared with fully dried aggregates and without being moisture conditioned; **Set 2** prepared with fully dried aggregates and being moisture conditioned; **Set 3** prepared with incompletely dried aggregates and without being moisture conditioned; and **Set 4** prepared with incompletely dried aggregates and being moisture conditioned. Superpave mix design specification was considered when preparing asphalt mixture and conducting dynamic modulus tests. Four replicate test specimens whose air void contents were controlled within  $7\pm 1\%$  were prepared for each of the proposed testing set such that adequate reliable measurements can be obtained and statistical calculations can be made. Among these four specimens, only three were selected for dynamic modulus tests, while the last one was kept as a reserve. The general test flow chart is shown in Figure 2.

### *Aggregate Preparation*

1. Since the new aggregates delivered from quarries in Herman, ME were wet, all the aggregates for testing were completely pre-dried before the starting of mixing and compaction.
2. In order to mimic the incomplete drying situation in asphalt plants, fully dried aggregates used for **Set 3** and **Set 4** were pre-soaked in CoreLok<sup>®</sup> bags with a volume of 10% of water by the mass of blended aggregates. The bags were sealed using CoreLok machine and placed them overnight to guarantee the complete soaking. The complete procedure has been described in Reference [3].
3. Before placing in an oven, all the aggregates prepared with and without soaking are supposed to be completely transferred to pans. For fully dried aggregates of **Set 1** and **Set 2**, the drying process was just a one-hour reheating process at the temperature of 90°C. However, under this temperature it would take more than four hours to control the moisture contents of those pre-soaking aggregates of **Set 3** and **Set 4** below 0.5%.

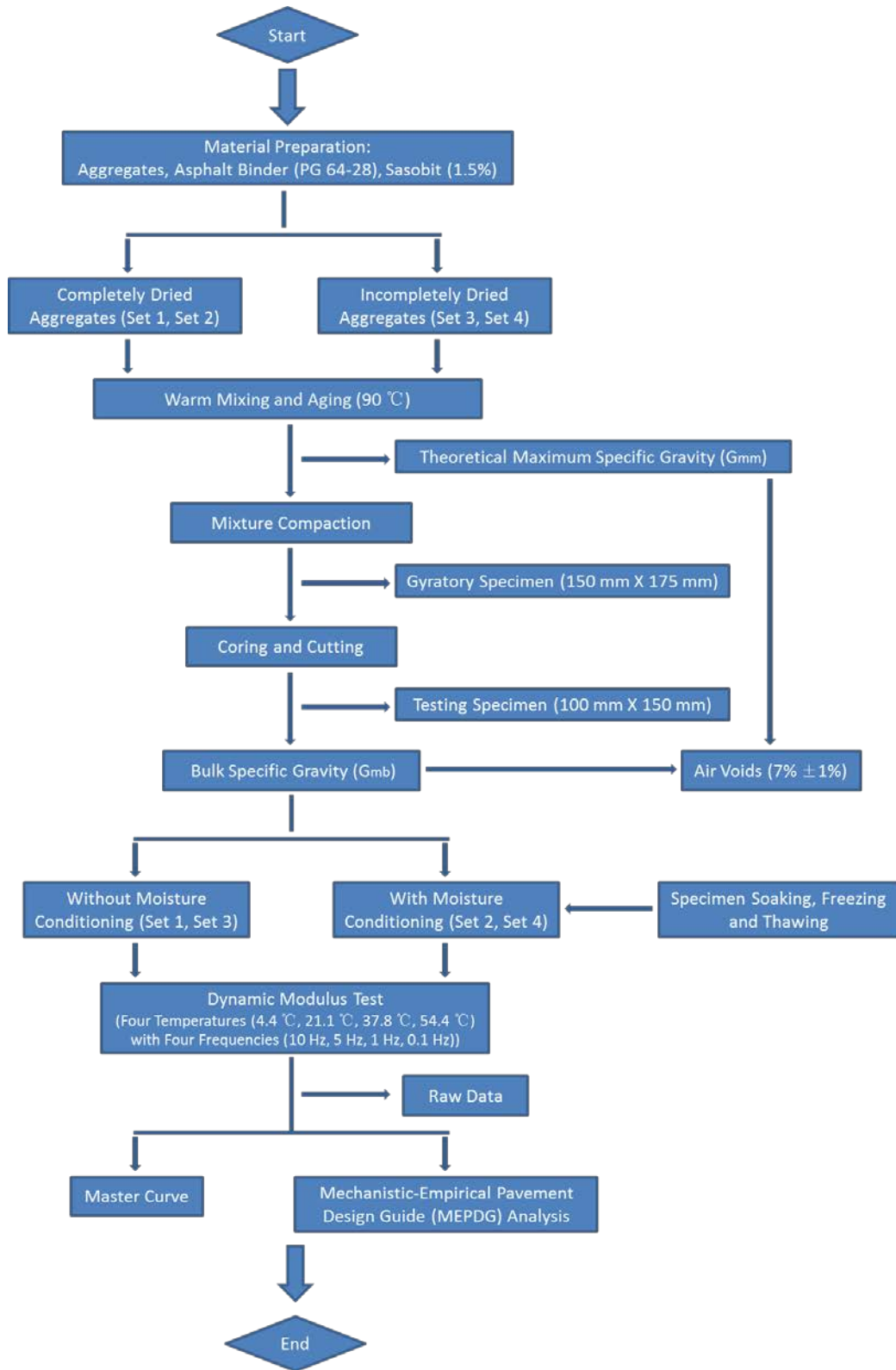


**Figure 2. General Flow Chart for Experimental Design**

### *Steps in Warm Mixing and Aging*

1. Remove one pan of aggregate samples from oven at a time and mix with modified PG 64-28 asphalt binder, which was heated to 125°C at least two hours before mixing. The mixing process was completed within strictly controlled time (two minutes) to avoid temperature loss or inadequate mixing.
2. After mixing in an industrial mixer, transfer loose mix back in pan and place back in the oven to age two hours at the temperature of 90°C.

### *Compaction Process*

1. When aging completed, the testing was performed to determine the theoretical maximum specific gravity ( $G_{mm}$ ) of the asphalt mixture according to the procedure provided by CoreLok. At least 2,000g of loose mixture made from the fully dried aggregates was used.
2. Based on the size and the air voids of gyratory specimens, the mass of loose mix was pre-calculated for one gyratory specimen and prepare a little more loose mix than the theoretical value consisting of loose aggregates and virgin asphalt binder in terms of specifications provided by Maine DOT for compaction due to the loss of mix during the mixing process. Table 3 summarizes the procedure of calculating the amount of loose mix that was required for filling the compaction mold.

**Table 3. Mass of Loose Mix for One Gyratory Specimen**

<b>Known Parameters</b>	Diameter, $D$ (mm)	Height, $H$ (mm)	Theoretical Maximum Specific Gravity, $G_{mm}$	Air Void Content, $A_v$	Surface Roughness Factor, $\alpha$
	150	175	2.398	8.5%	0.98
<b>Calculated Parameters</b>	Bulk Specific Gravity, $G_{mb}=(1-A_v)^* G_{mm}$	Density (g/mm <sup>3</sup> ), $\rho=G_{mb}/1000$	Volume (mm <sup>3</sup> ), $V=\pi*(D/2)^2*H$	Mass (g), $M=V*\rho$	Actual mass (g), $M'=M*\alpha$
	2.194	0.002194	3091157	6782	6646

*Note: 8.5% refers to the air void content of the gyratory specimen rather than that of the test specimen after coring and cutting since the test specimen removed from the middle of the gyratory specimen would be subjected to a higher stress and the air void content of the test specimen is 1.5 to 2.5 percent lower than that of the gyratory specimen [17].*

3. Remove loose mixture from the oven and scoop calculated mass of mixture into the

mold with the diameter of 150 mm. Place the mold in a Superpave gyratory compactor to automatically conduct compaction. The height-control mode was used in accordance with AASHTO T 312 “Standard Method of Test for Preparing and Determining the Density of Hot Mix Asphalt (HMA) Specimens by Means of the Superpave Gyratory Compactor”. Figure 3 shows four photos of the process of warm mixing and compaction.



**Figure 3. Warm Mixing and Compaction Process**

(1. Oven; 2. Mixer with mixing bowl and paddle; 3. Superpave gyratory compactor and compaction mold; 4. Finishing gyratory specimen)

### ***Test Specimen Fabrication***

1. The target dimension of the test specimen performed in dynamic modulus test is 101.6 mm (4 in.) diameter by 152.4 mm (6 in.) tall in accordance with specifications of NCHRP 9-29.
2. Drill a nominal 4 in. diameter core from the center of the gyratory specimen using a 4 in. coring rig. Cut the rough ends of the core to obtain a nominal 6 in. height test specimen using a double blade saw. The devices of coring and cutting as well as specimens after fabrication are presented in Figure 4.
3. Test specimens would be all wet since water was introduced during coring and cutting process to alleviate the abrasion of rig and blades. Thus, air void content cannot be measured using CoreLok until test specimens are subjected to the drying process in front of a fan for more than three days. The target air void content of the final test specimen must be controlled between 6%-8%. Reject specimens with air voids beyond the range of the target air void.

4. If test specimens will not be tested for dynamic modulus tests within 24 hours, ziplock bags are used to wrap them and they are stored in an environmentally protected storage area at temperatures between 40°F and 80°F [17].



**Figure 4. Coring and Cutting Process**

(1. Device of coring; 2. Specimen after coring; 3. Device of cutting;  
4. Specimen after cutting)

### ***Moisture Conditioning***

1. Test specimens of **Set 3** and **Set 4** were subjected to one freeze-thaw cycle before conducting dynamic modulus tests.
2. Steps in freeze-thaw cycle: I. Specimen soaking: enclose specimens in bags and seal them using CoreLok; submerge bags in the water and cut them open; let specimens soak in water for half hours. II. Specimen freezing: remove specimens from water and seal them in bags again; place bags in a freezer with a temperature setting of  $-28\pm 3^{\circ}\text{C}$

for 24 hours. III. Sample thawing: after freezing, remove specimens to a water tank with the temperature of 60°C and condition in the circulating water for no less than 48 hours. Figure 5 shows the freeze-thaw conditioning process.

3. Specimens were put in ziplock bags immediately after conducting moisture conditioning process.



**Figure 5. Freeze-thaw Cycle**

(1. Freezing in a freezer; 2. Thawing in a hot water tank)

### 3.3 Dynamic Modulus Test

The dynamic modulus testing of this project was conducted according to NCHRP 9-29 [7]. However, a little change was made to perform a better test. Four temperatures (4.4, 21.1, 37.8, 54.4°C) under four loading frequencies (10, 5, 1, 0.1 Hz) were used in this test.

Each test specimen could not be placed in the Universal Testing Machine (UTM) environment chamber until mounting studs for two axial LVDTs were already instrumented on the sides of the specimen using quick setting epoxy. A specimen with mounting studs and the device for dynamic modulus tests are shown in Figure 6.

Each test specimen should be tested from the lowest temperature to the highest, while at a given temperature specimens should begin with the highest loading frequency and proceed to the lowest. It's supposed to test all frequencies before moving to the next highest temperature. A dummy specimen with a thermocouple inserted in the center can be monitored to determine when the specimen reaches the target test temperature.



Temperature and temperature equilibrium time used in this project are listed in Table 4.



**Figure 6. Dynamic Modulus Test**

(1. Specimen with mounting studs; 2. Device for dynamic modulus test)

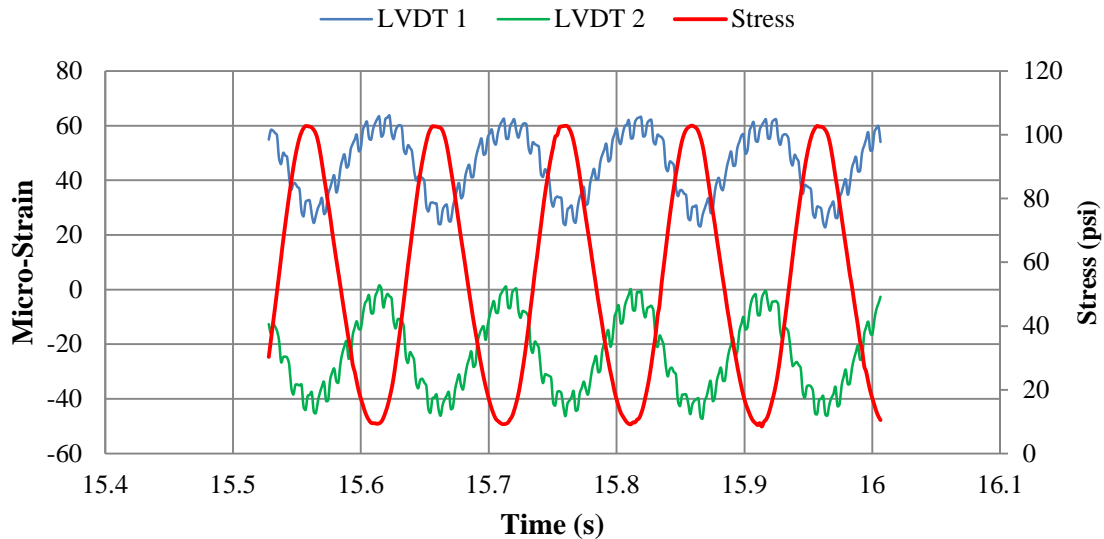


**Figure 7. Specimen Test Results of Dynamic Modulus Test**

(Stress (1 curve) and strain (2 curves) in dynamic loading using 10 Hz frequency at the temperature of 4.4°C)

Three test specimens for each set were used to conduct dynamic modulus tests at four different temperatures and four loading frequencies. Essentially sinusoidal loading applied to specimens from different sets at each temperature were determined to ensure recoverable strains between 50 and 150 microstrain in the specimens. The load stress

levels in this project are summarized in Table 5.

The ShedWorks<sup>®</sup> software was used as the data acquisition program to automatically record testing data and create a Microsoft Excel worksheet. The data contained readings of the LVDTs at each frequency, which were then utilized to determine the dynamic modulus and phase angle by a MatLAB<sup>®</sup> program developed at WPI [23]. The MatLAB code can be found in Appendix F. Figure 7 shows a typical set of results from the  $E^*$  test.

**Table 4. Temperature Equilibrium Time for  $E^*$  Test**

Test Temperature (°C)	Temperature Equilibrium Time from Room Temperature (Hour)
4.4	Overnight
21.1	2
37.8	4
54.4	7

**Table 5. Dynamic Modulus Testing Loads**

ID	Temperature (°C(°F))	Frequency (Hz)	Peak Load (lb)	Contact Load (lb)
Set 1	4.4 (40)	10, 5, 1, 0.1	1300	65
	21.1 (70)	10, 5, 1, 0.1	450	23
	37.8 (100)	10, 5, 1, 0.1	200	10
	54.4 (130)	10, 5, 1, 0.1	50	5
Set 2	4.4 (40)	10, 5, 1, 0.1	600	30
	21.1 (70)	10, 5, 1, 0.1	200	10
	37.8 (100)	10, 5, 1, 0.1	50	5
	54.4 (130)	10, 5, 1, 0.1	30	5
Set 3	4.4 (40)	10, 5, 1, 0.1	1000	50
	21.1 (70)	10, 5, 1, 0.1	250	13
	37.8 (100)	10, 5, 1, 0.1	50	5
	54.4 (130)	10, 5, 1, 0.1	30	5
Set 4	4.4 (40)	10, 5, 1, 0.1	500	25
	21.1 (70)	10, 5, 1, 0.1	150	8
	37.8 (100)	10, 5, 1, 0.1	45	5
	54.4 (130)	10, 5, 1, 0.1	25	5

**Note:** *Set 1* prepared with fully dried aggregates and without being moisture conditioned; *Set 2* prepared with fully dried aggregates and being moisture conditioned; *Set 3* prepared with incompletely dried aggregates and without being moisture conditioned; and *Set 4* prepared with incompletely dried aggregates and being moisture conditioned (the same in the following tables and

*figures).*

## 4. Results and Analysis

### 4.1 Control of Moisture to Achieve Incomplete Drying

What is incomplete drying? There is no exact definition and quantitative standard in any literature. As long as the moisture content is above zero, the aggregates can be regarded as incompletely dry. As to aggregates prepared for mixing with asphalt binder, there is no doubt that complete dry will be the most ideal situation, which enables perfect coating and good field performance. However, in the asphalt industry, whether it is a batch plant or a drum plant, it is hard to guarantee complete drying of aggregates, and it is more so in the case of Warm Mix Asphalt.

In this project 0.5% of moisture content was selected as the critical value to differentiate able-to-mixing and unable-to-mixing for incompletely dried aggregates of **Set 3** and **Set 4**. When moisture content decreases to the level of 0.5%, water can hardly be seen on the surface of aggregates, which probably indicates a good condition for asphalt coating. At this moisture content and below, most of the residual moisture probably stays inside of the aggregates. The general procedure of controlling incompletely drying is as follows: firstly, pre-calculate the mass of incompletely dried aggregates with 0.5% moisture content retained; secondly, check the mass of aggregates every half hours; thirdly, pour the aggregates from pan to mixing bowl until the mass is close to the target mass (the difference is not more than 100g); finally, mix the aggregates with asphalt binder when moisture content has decreased to 0.5%. Table 12 and Table 13 in Appendix A are presented the descending order of the aggregate mass of **Set 3** and **Set 4** every half hour, respectively. Curves of the mass change are also plotted in Figures 8 through 11.

At the beginning of the drying process, the second pan was placed in the oven half hour later than the first pan (two used 4 hours and the other two used 4.5 hours as shown in tables), the purpose of which was to ensure that the two pans of aggregates were able to mix with asphalt binder with 0.5% moisture content. Even though such preparations and considerations were made, by the end of the drying process, it was not possible to get 0.5% all the time (moisture content ranged from 0.29% to 0.5% of eight mixtures from the tables). The primary reason is that water is lost by evaporation also. As figures show, the rates of water evaporation in the first three hours are generally linear and even, while in the last hour the rates decrease significantly. It's probable that the mixing bowl diminished the interface of aggregates and air resulting in obstructing water evaporation.

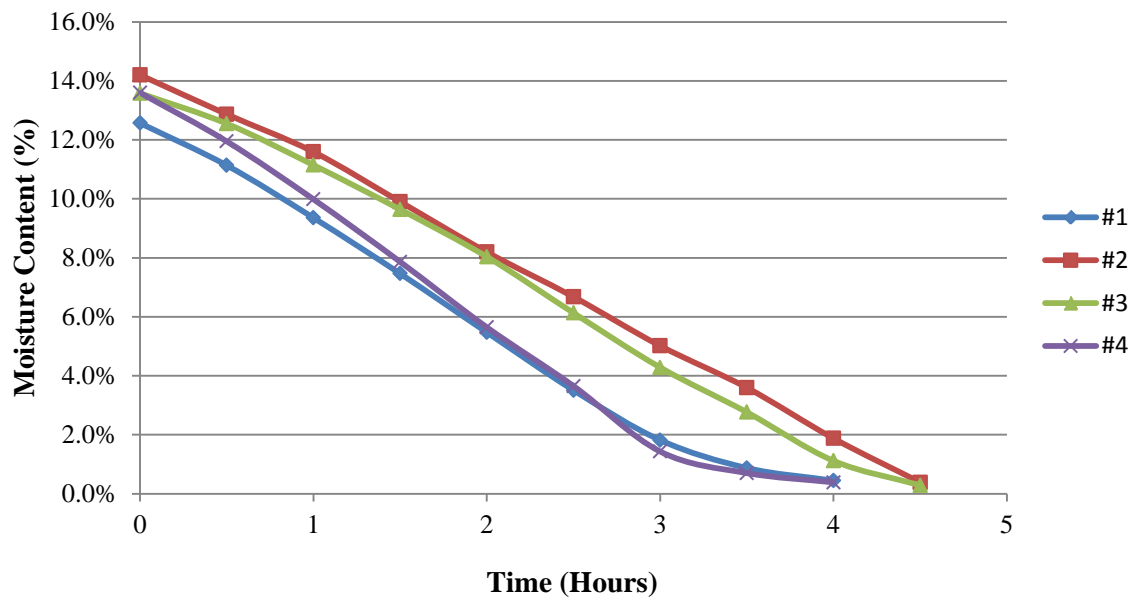


**Figure 8. Moisture Contents of Set 3**

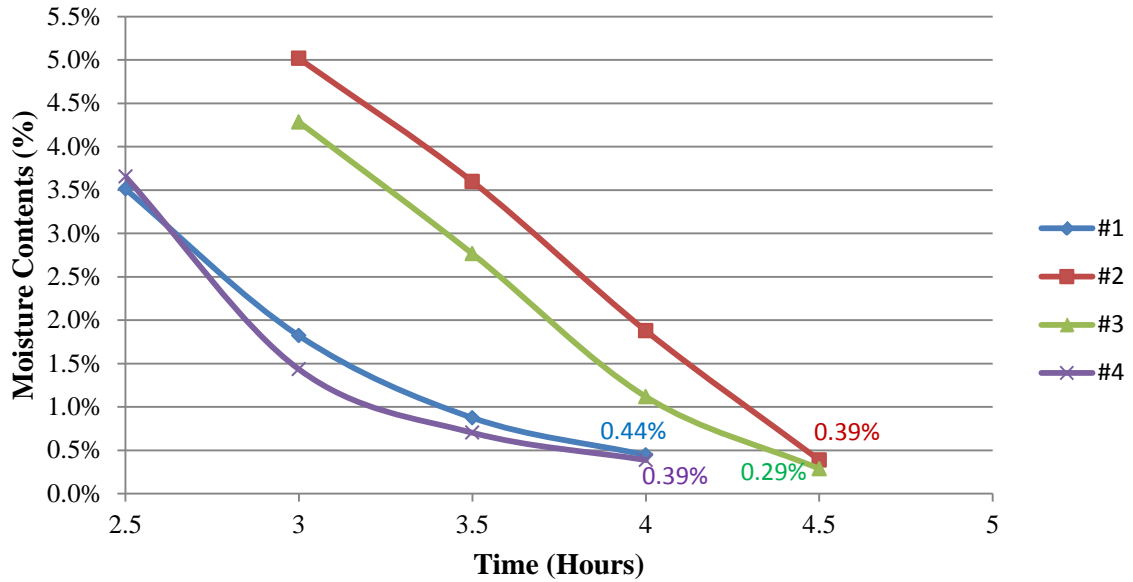


**Figure 9. Moisture Contents (Last 2 Hours) of Set 3**

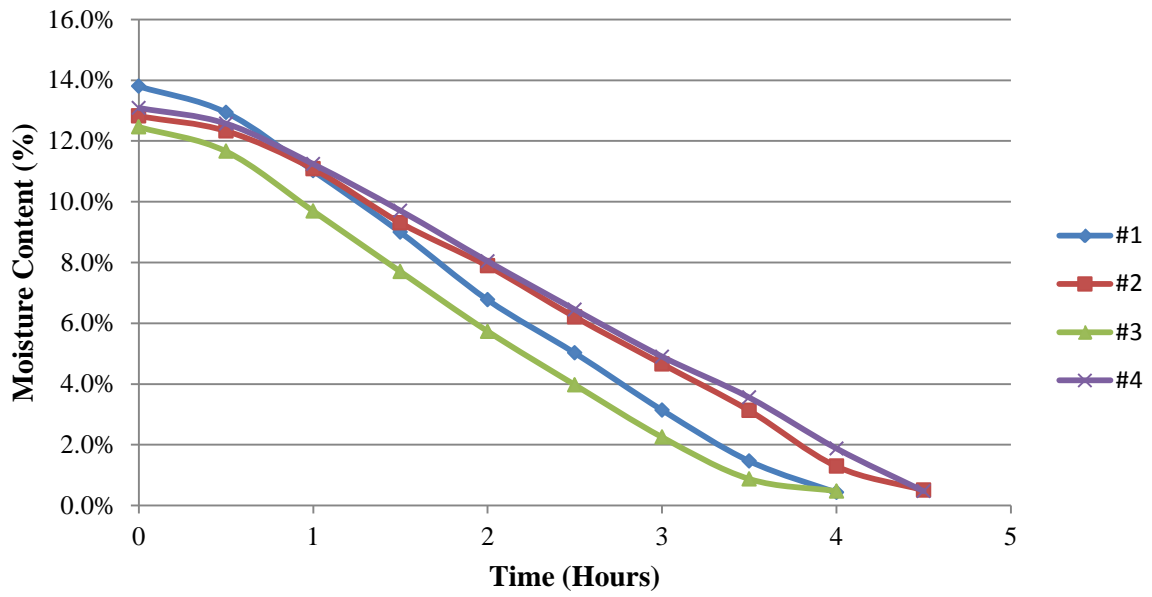


**Figure 10. Moisture Contents of Set 4**

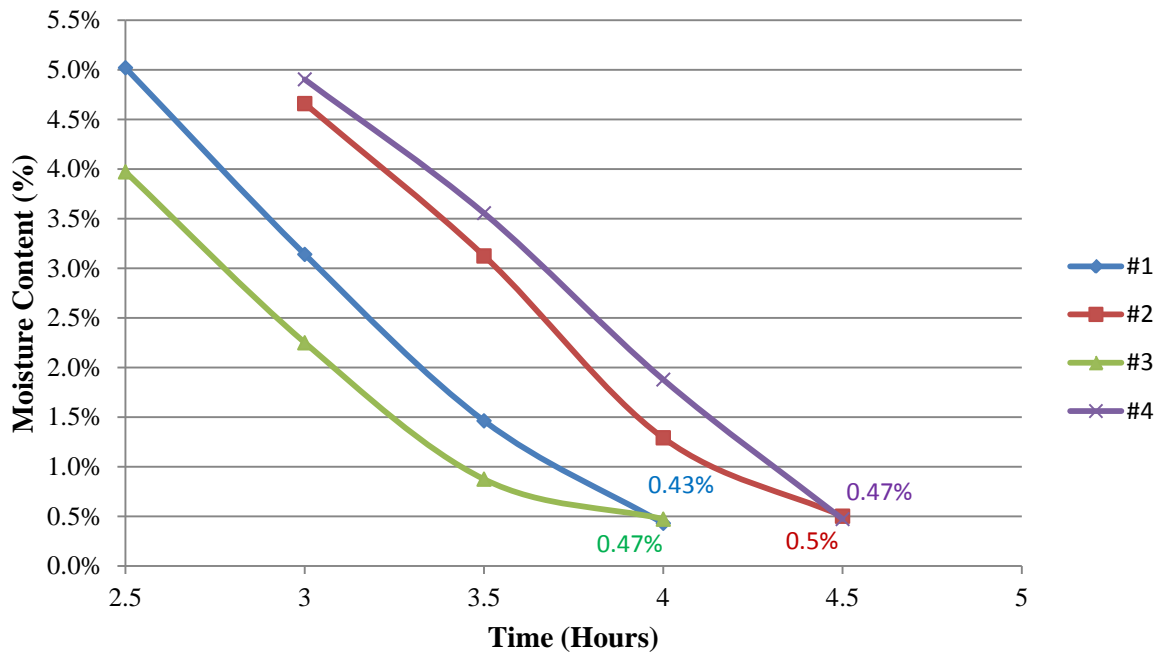


**Figure 11. Moisture Contents (Last 2 Hours) of Set 4**

## 4.2 Volumetric Properties

Before conducting mechanical tests, air void content or voids in total mix (VTM) of the samples were evaluated to determine variations, if any. Theoretical maximum specific gravity ( $G_{mm}$ ) and bulk specific gravity ( $G_{mb}$ ) are two prerequisite parameters to calculate VTM of a certain specimen. In this project,  $G_{mm}$  was measured as 2.398 and each specimen had its own  $G_{mb}$ , which can be used to obtain VTM. The VTM values for the specimens in this research were in a range of 6%-8%. Note that only VTM of test specimens were determined rather than the gyratory specimens whose VTM had been pre-set as 8.5%. The VTM results for specimens tested are presented in Figure 12 by type of different sets. The raw data of  $G_{mm}$ ,  $G_{mb}$  and VTM can be found in Tables 14 through 19 in Appendix B.

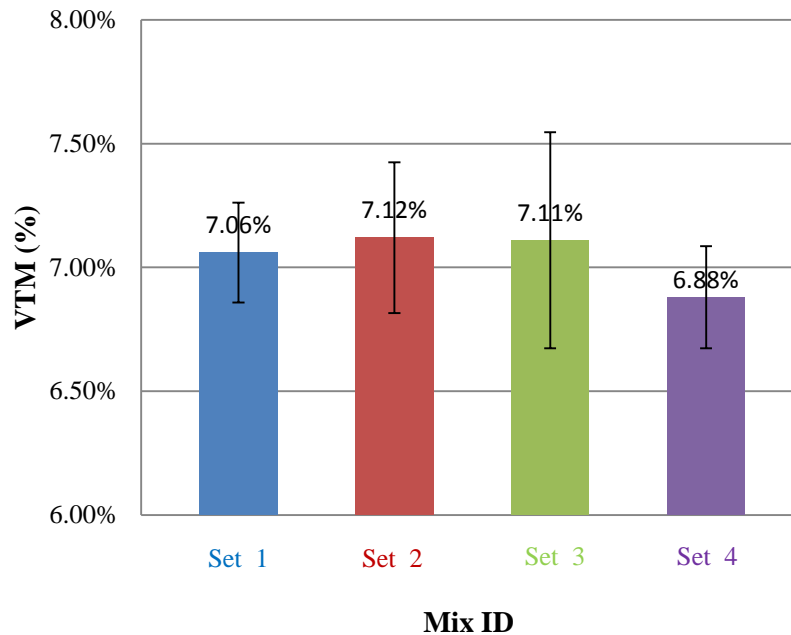


**Figure 12. Void in Total Mix (VTM) for Dynamic Modulus Tests**

It is clear that all sets of specimens were within the target VTM. Even if VTM of all the gyratory specimens were around 8.5%, after coring and cutting VTM of test specimens were still in a range between 6.55% and 7.62%. And there is no sign that incompletely drying aggregates had any significant influence on VTM of specimens.

## 4.3 Dynamic Modulus Test and Master Curve

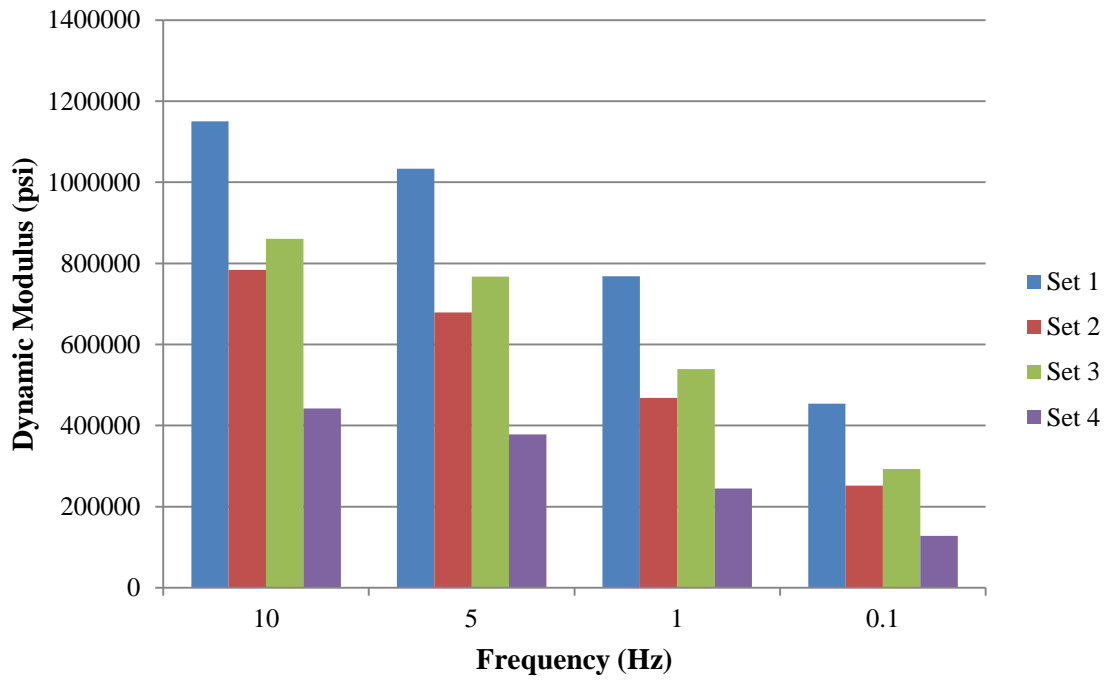
### 4.3.1 Dynamic Modulus and Phase Angle Results

As mentioned earlier, NCHRP 9-29 was followed to perform the dynamic modulus test using an UTM machine. This test was conducted to investigate the difference between dynamic modulus of complete-dry and incomplete-dry as well as with-moisture-conditioning and without- moisture-conditioning mixes. Data of dynamic modulus and phase angle were reduced by MatLAB program at four temperatures (4.4, 21.1, 37.8 and 54.4°C) with four loading frequencies (10, 5, 1 and 0.1Hz) at each temperature. A total of three replicate specimens for each set were tested at each temperature and loading frequency. Table 20 in Appendix C shows the summary of the average values of the dynamic modulus and phase angle.

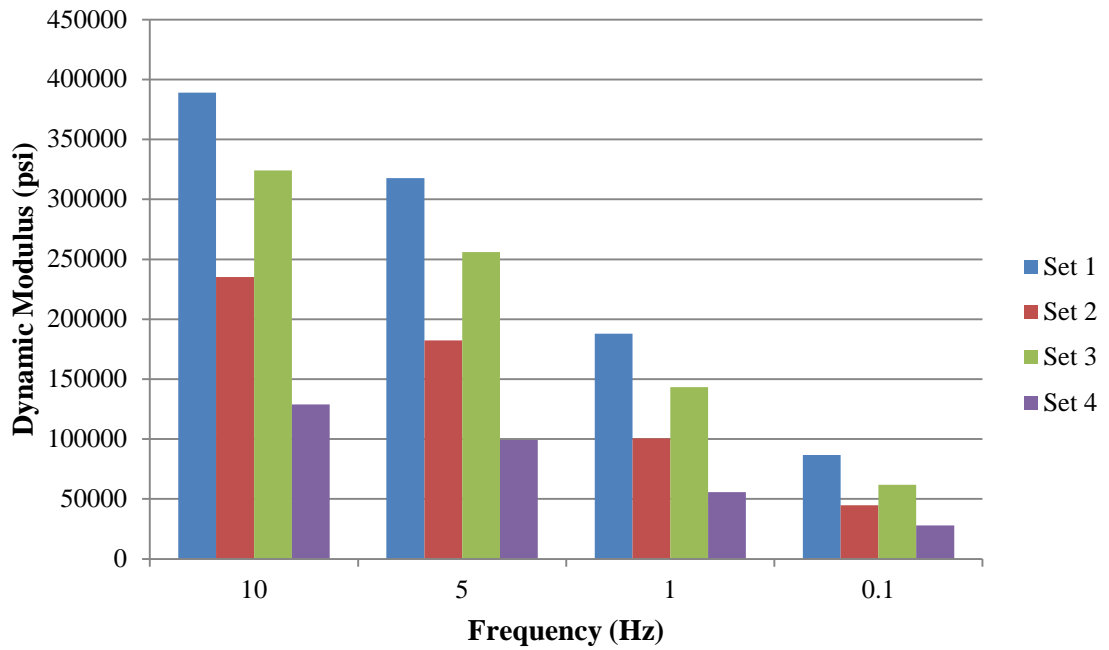
As expected, the test results showed mixes of each set had the gradually decreasing trend of dynamic modulus with increasing temperatures, with the highest values being 4.4°C. Also dynamic modulus was the maximum at the highest frequency and decreased with a decrease in frequency, except for certain outliers that are marked with red font in the tables. But phase angle results had higher variability. It is noted from Table 20 that the phase angles increased up with the decreasing of frequencies. At 21.1°C, **Set 1** still kept this rule and **Set 3** basically followed the increased trend; whereas, values in **Set 2** were varied and in **Set 4** this trend was reversed. For temperatures of 37.8°C, phase angle generally began to decrease from higher frequency to lower one. However, at the temperature of 54.4°C, this decreasing is not so obvious; it could be that at this temperature, the predominant effect was from the aggregate interlock rather than from the asphalt binder [19, 24].

Mixes from **Set 1** had the highest dynamic modulus values followed by those from **Set 3**, **Set 2** and **Set 4**. The results demonstrated that moisture does influence the dynamic modulus negatively and moisture conditioning had more effect than incomplete drying. **Set 1** had the lowest phase angle values compared with the highest ones of **Set 4**, which has been moisture conditioned with incompletely dried aggregates. The comparisons of dynamic modulus of each set at different temperatures are presented in Figures 13 through 16 in Appendix C by frequency. The results of phase angle are also shown in Figures 17 through 20 in Appendix C.

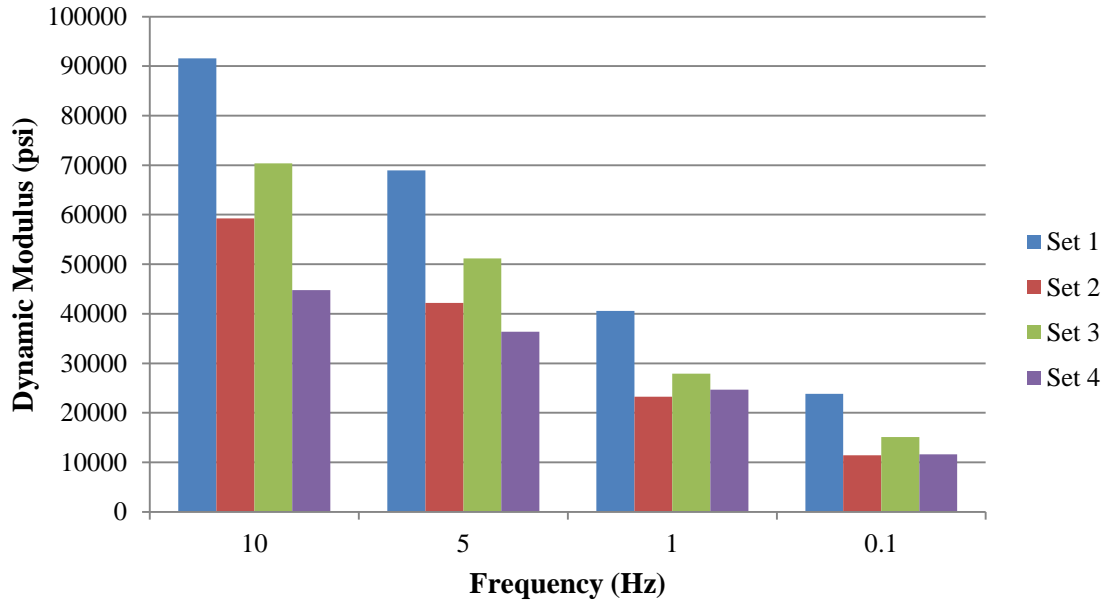




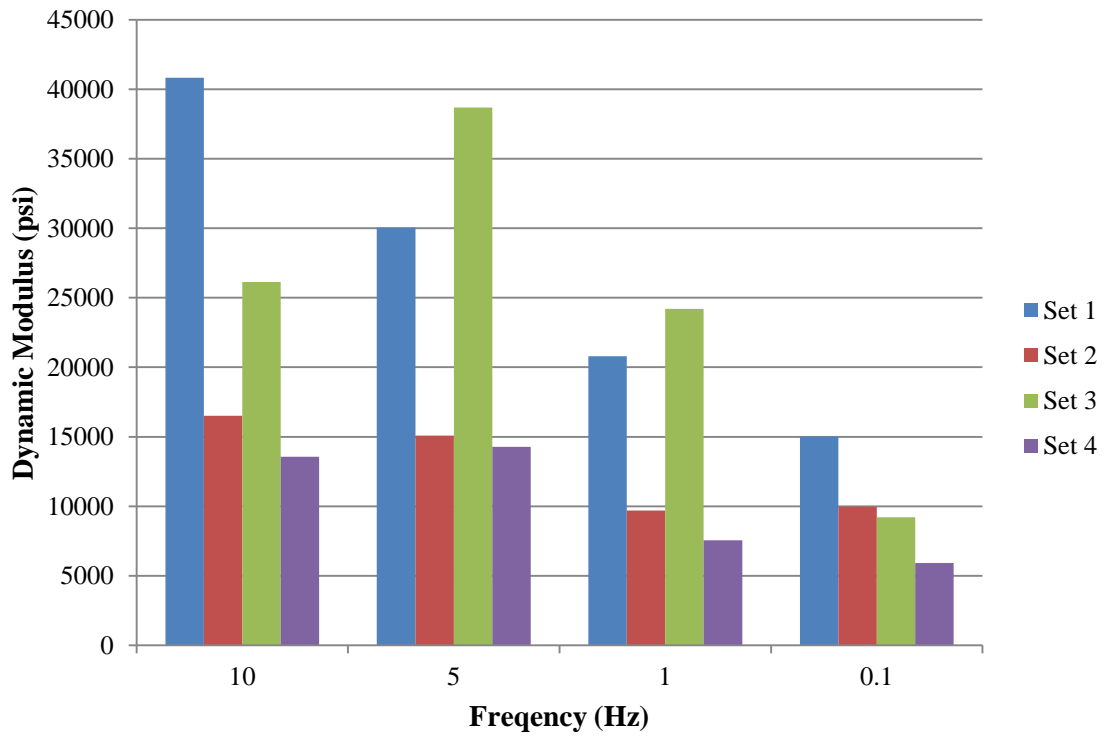
**Figure 13. Dynamic Modulus Results at 4.4°C**



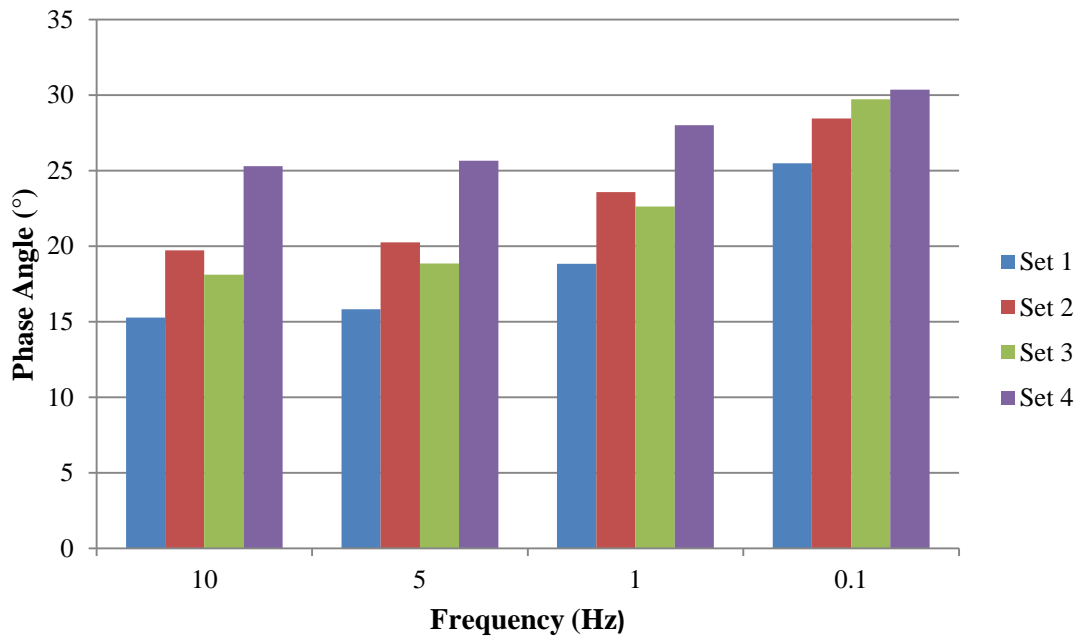
**Figure 14. Dynamic Modulus Results at 21.1°C**



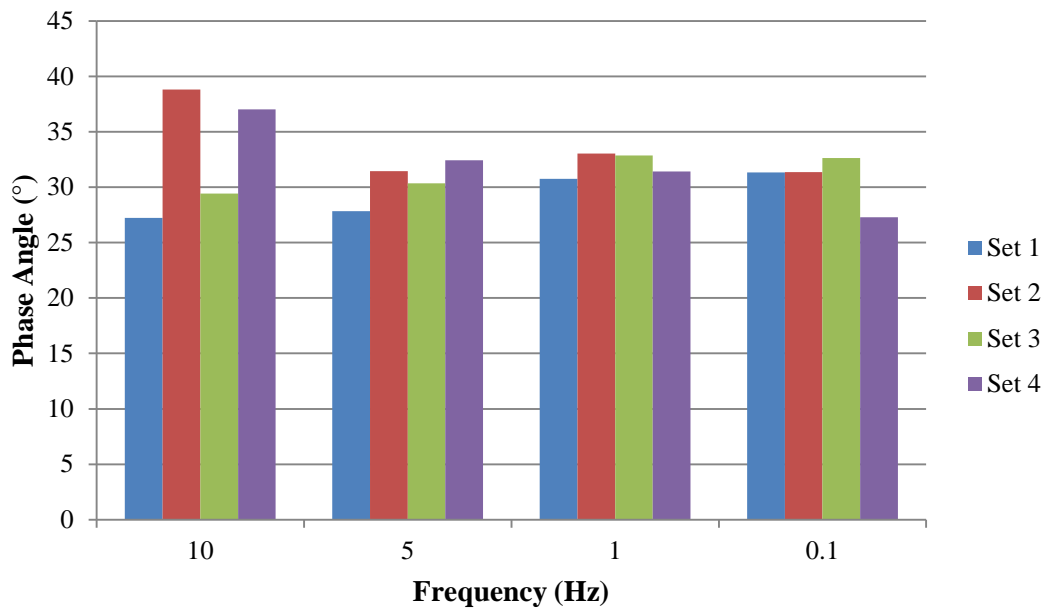
**Figure 15. Dynamic Modulus Results at 37.8°C**



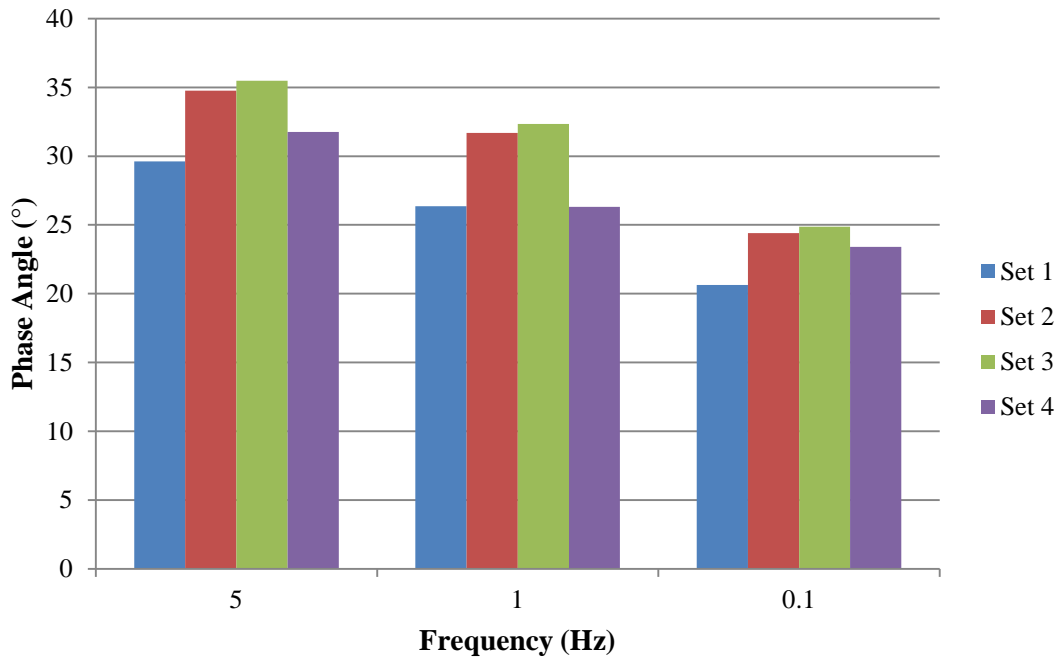
**Figure 16. Dynamic Modulus Results at 54.4°C**



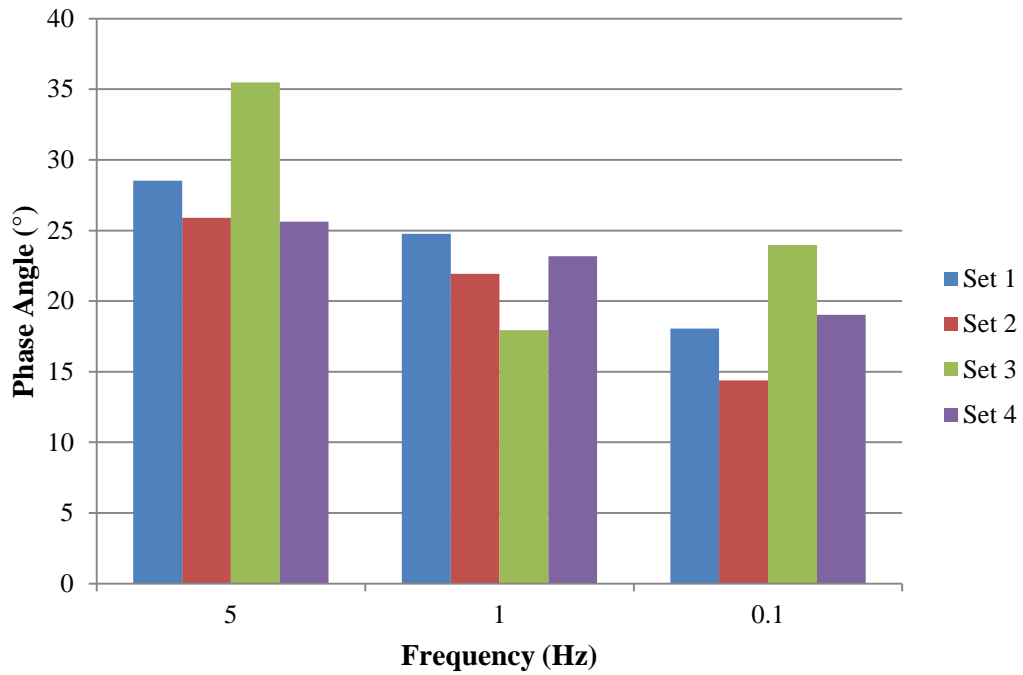
**Figure 17. Phase Angle Results at 4.4°C**



**Figure 18. Phase Angle Results at 21.1°C**



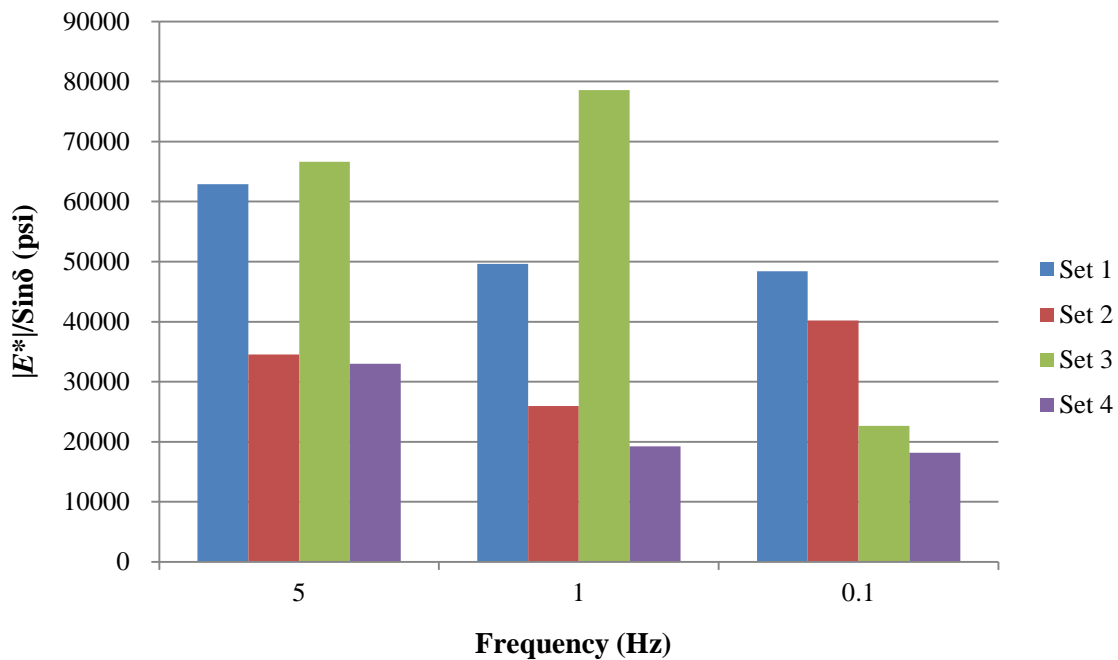
**Figure 19. Phase Angle Results at 37.8°C**



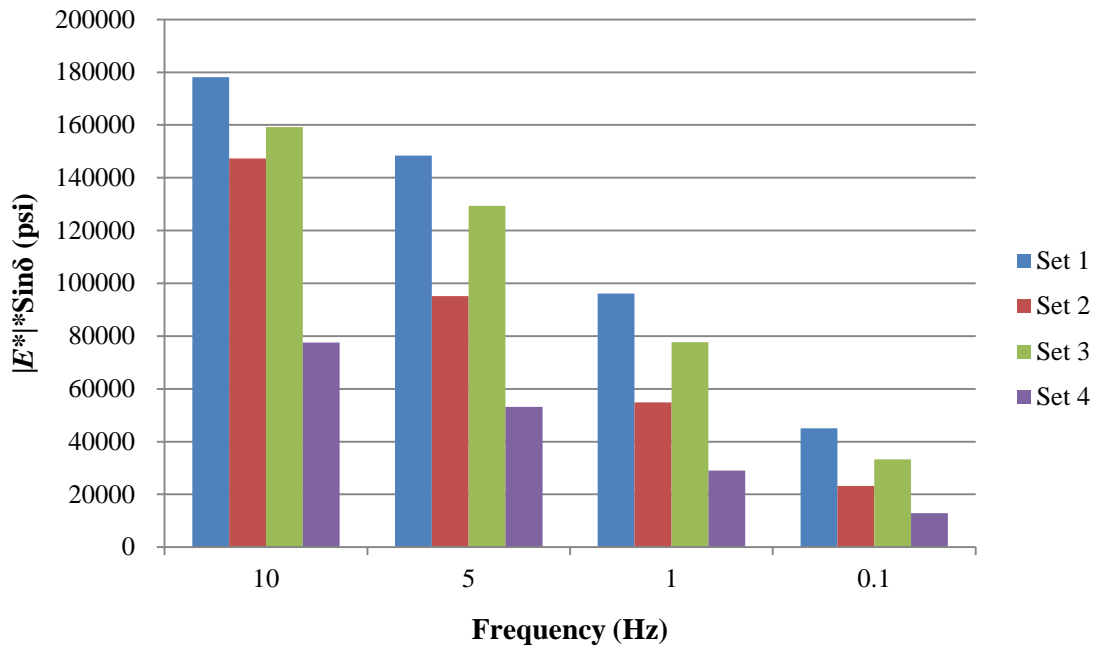
**Figure 20. Phase Angle Results at 54.4°C**

As mentioned previously, apart from  $E^*$  itself that can differentiate the quality of the mixture,  $|E^*|/\sin\delta$  measured at high temperature and  $|E^*|\sin\delta$  acquired at intermediate temperature are also associated with rutting susceptibility and fatigue resistance of the mixture, respectively. In terms of Table 20, values of  $|E^*|/\sin\delta$  and  $|E^*|\sin\delta$  were calculated and listed in Table 21. Furthermore, the comparisons of  $|E^*|/\sin\delta$  at 54.4°C and  $|E^*|\sin\delta$  at 21.1°C among different sets are plotted in Figure 21 and Figure 22, respectively.

Again, red numbers in Table 21 represented outliers which were not used for plots. The most likely reason of those outliers is the structural instability of the asphalt mixture at high temperature with high frequency. Another reason could be that the glued gage points may loosen at this high temperature, particularly when the gage points were attached to the matrix of fine aggregates which were moisture conditioned. However, at intermediate temperature of 21.1°C, the trend of  $|E^*|\sin\delta$  was relatively much better.



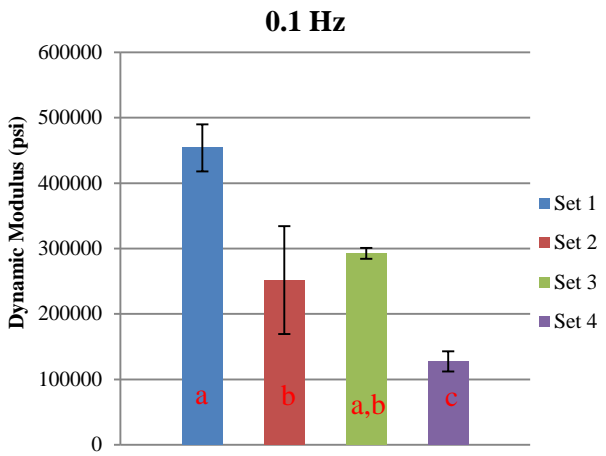
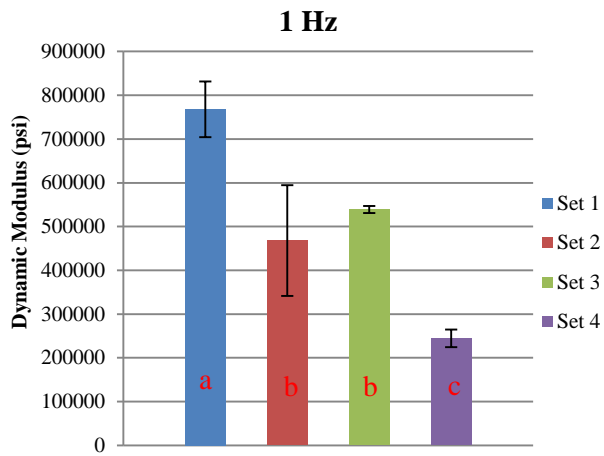
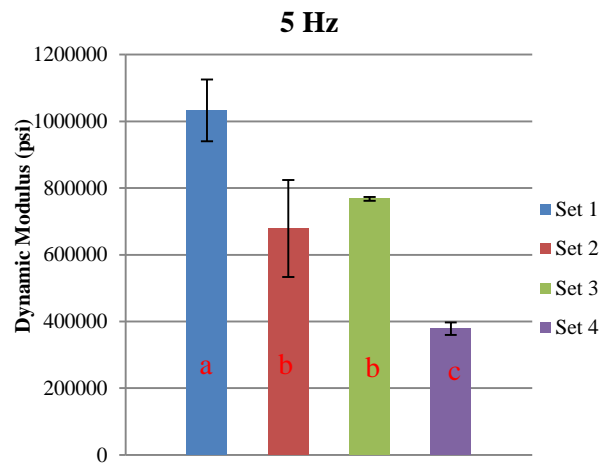
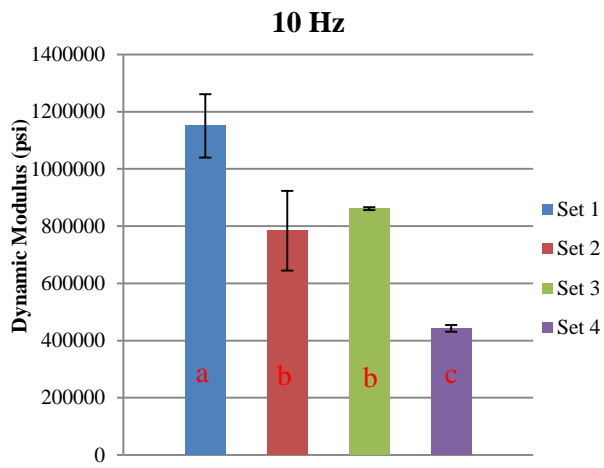
**Figure 21.  $|E^*|/\sin\delta$  Results for 54.4°C**



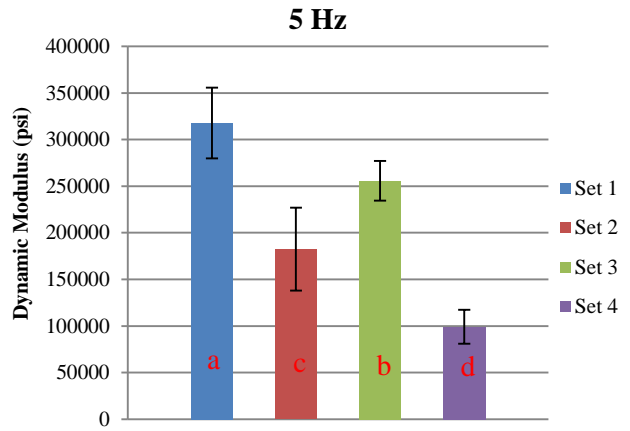
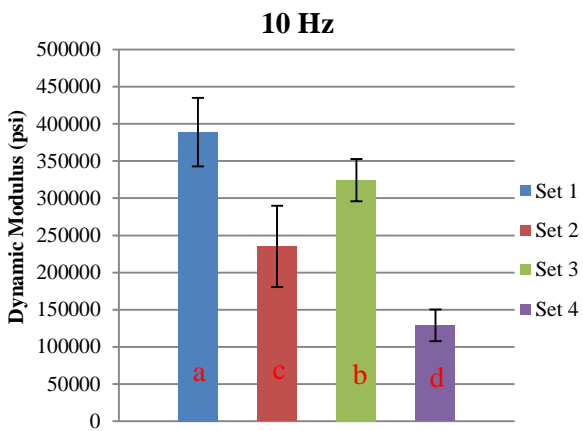
**Figure 22.  $|E^*| \sin \delta$  Results for 21.1°C**

### 4.3.2 ANOVA for Dynamic Modulus Results

The ANOVA, short for analysis of variance, is a series of statistical tests used to determine whether or not the means of several groups are all equal (or significantly different). In this study, with the purpose of understanding the difference of dynamic modulus results among groups at certain temperature, the ANOVA was carried out utilizing Statistical Package for the Social Sciences (SPSS) software version 19.0. The linear model and *post hoc* testing method was employed to conduct ANOVA analysis. Considering the heterogeneous nature of the group variances and small sample sizes, Student-Newman-Keuls (SNK) statistical model included in *post hoc* method was selected to determine whether there were significant differences among testing groups. The ANOVA results at the temperatures of 4.4, 21.1 37.8°C are shown in Figure 23 through 25, each of which is consisted of four subplots by type of frequencies. The raw data of ANOVA can also be found from Table 30 to Table 32 in Appendix D. Note that the lowercase letters (*a*, *b*, *c* and *d*) stand for differences among groups, that is, if two groups are significantly different, they belong to two distinct lowercase letters. Analysis of 54.4°C was not included owing to the unreliable data obtained.



**Figure 23. ANOVA Analysis at 4.4°C**



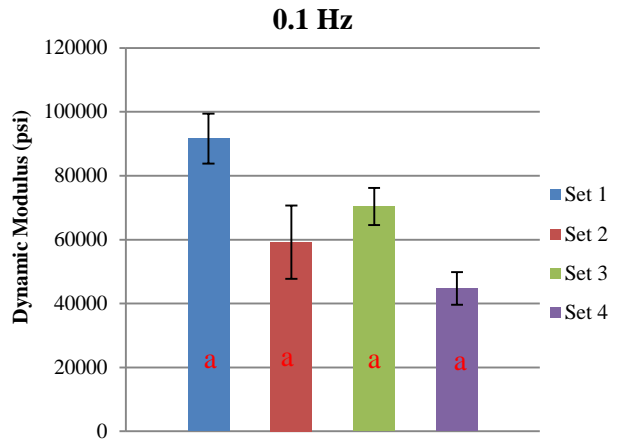
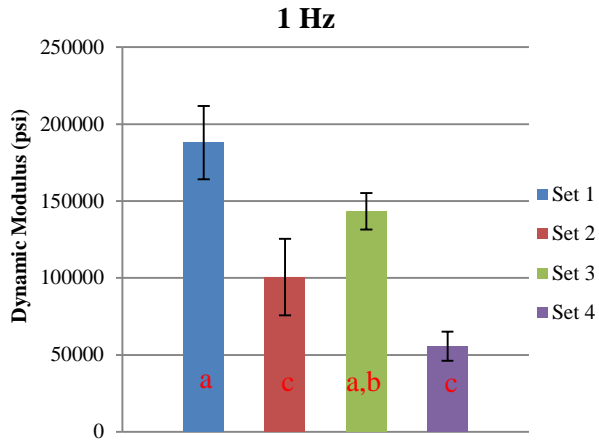


Figure 24. ANOVA Analysis at 21.1°C

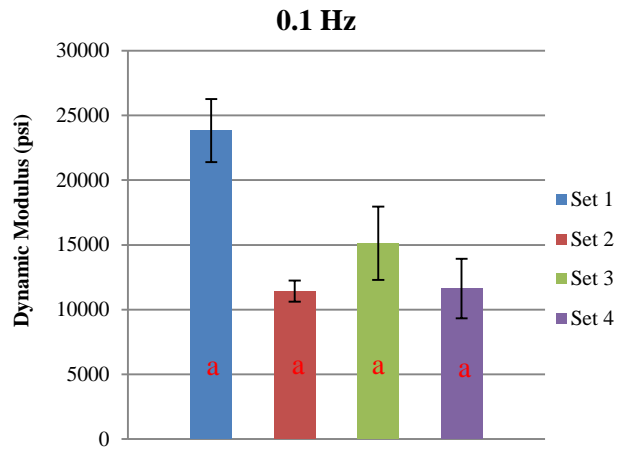
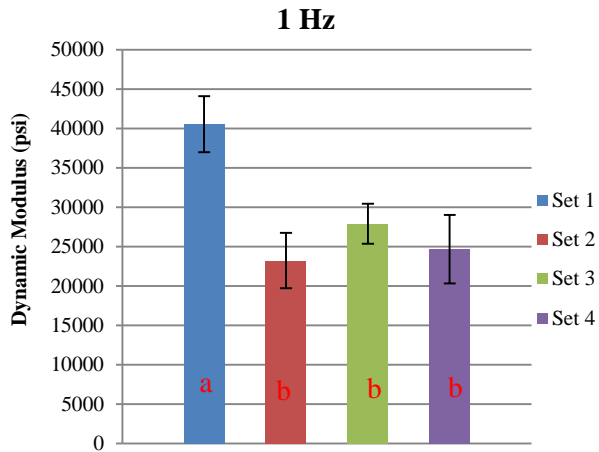
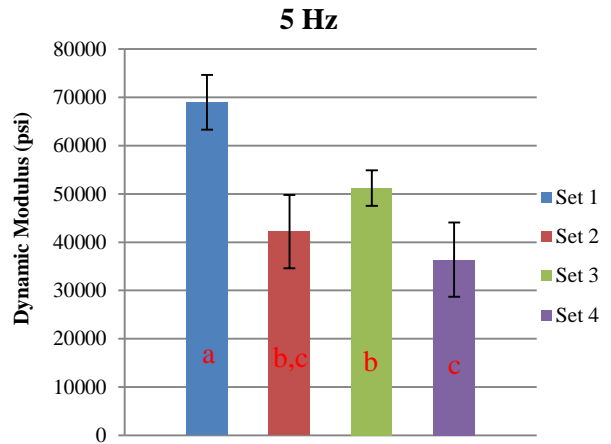
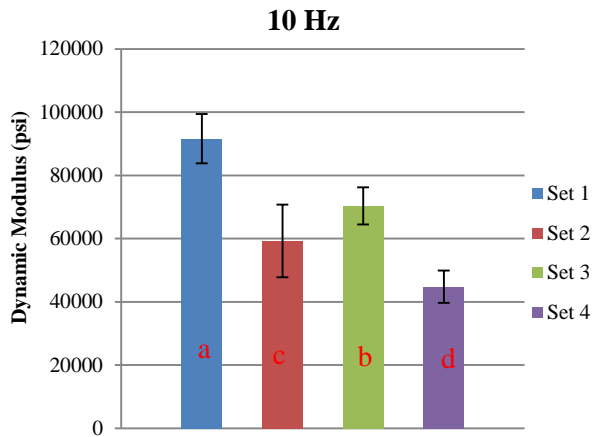


Figure 25. ANOVA Analysis at 37.8°C



The results of ANOVA analysis were procured based on the SNK tables in Appendix D. Significance level of 0.05 was used during the analysis, which means the confidence intervals are 95.0%. The meaning of variance numbers of SNK tables from 1 to 16 is interpreted in Table 6.

**Table 6. The Meaning of Variance Numbers**

<b>Frequency</b>	<b>Set 1</b>	<b>Set 2</b>	<b>Set 3</b>	<b>Set 4</b>
<b>10 Hz</b>	<i>1</i>	<i>5</i>	<i>9</i>	<i>13</i>
<b>5 Hz</b>	<i>2</i>	<i>6</i>	<i>10</i>	<i>14</i>
<b>1 Hz</b>	<i>3</i>	<i>7</i>	<i>11</i>	<i>15</i>
<b>0.1 Hz</b>	<i>4</i>	<i>8</i>	<i>12</i>	<i>16</i>

According to figures of three temperatures shown above, analysis for each temperature can be made as follows:

1. At the temperature of 4.4°C, the difference of **Set 1** and **Set 4** are significant regardless of frequencies. **Set 2** and **Set 3** can be regarded as in the same group, which means there is no significant difference. In other words, incomplete drying and moisture conditioning have the similar effect on dynamic modulus results at the lowest temperature of 4.4°C no matter what the frequency is.
2. At the temperature of 21.1°C, significant differences are among four groups at the frequency of 10Hz and 5 Hz. At 1 Hz, **Set 3** and **Set 4** can be regarded as in the same group. However, four sets cannot be differentiated clearly at the lowest frequency of 0.1 Hz.
3. At the temperature of 37.8°C, the differences among four sets are still significant at 10 Hz. But from 5 Hz to 1 Hz, the differences among **Set 2**, **Set 3** and **Set 4** tend to be insignificant. And at the lowest frequency of 0.1 Hz like the situation of 21.1°C, all sets can be summarized in one group, which means moisture has no effect on dynamic modulus results on such condition.

### **4.3.3 Development of Master Curve**

According to the description of Simple Performance Test in the specification of NCHRP 9-29, master curves in this research were established with the aid of Hirsch model. This model differs from other predictive models mainly because it utilizes shear modulus of binder and volumetric properties of mixtures to calculate the limiting maximum  $|E^*|$  before predicting the master curve. This approach is able to obtain more reasonable and accurate estimating results at very low and very high frequencies in a small range of

temperatures. In this project, three temperatures (4.4°C, 21.1°C and 37.8°C) were selected to construct master curves. Standard deviations of dynamic moduli of each set are presented from Table 22 to Table 25 in Appendix C in order to demonstrate why  $E^*$  values at 54.4°C were not employed for master curves. Again, red numbers indicate irregular results. Obviously, values of Std./Ave. of  $E^*$  at 54.4°C are much greater than those at other temperatures, which indicates the highest temperature is not reliable for predicting master curves.

Three temperatures with four frequencies of each set were employed to perform data reduction and optimization to construct master curves. Parameters and the calculating procedures are presented in the computational Tables 26 through 29 in Appendix C. Red numbers marked in tables refer to iterative and optimized parameters that were plugged into Equation 6 to calculate predictive  $E^*$  values. The fitting curves of predicted  $E^*$  values and measured  $E^*$  values as well as the corresponding shift factor plots can be found in Figure 26 to 29.  $R^2$  of four sets were observed to be close to 1, which means Hirsch model is effective in predicting  $E^*$  from measured values and then constructing master curves.

Dynamic modulus master curve of four-set mixtures is summarized in Figure 30. The reference temperature of 21.1°C (70°F) was employed to establish the master curve. The data at the other two temperatures were shifted with respect to log of reduced time until the curves merge into a single smooth function. Therefore, the resulting dynamic modulus master curve, as a function of time, depicts the time dependency of the material. In this figure, two dash lines at the top and bottom of curves are respectively indicative of the maximum and minimum of dynamic modulus that four mixtures could reach at a wide range of frequencies. Theoretically, curves should be in a sequence of **Set 1**, **Set 3**, **Set 2** and **Set 4** from top to bottom based on the mechanical performance. From this figure, it can be noticed that every curve appears in a good shape separately, but the fourth curve locates between the first and the third one at high log of reduced time, i.e., at high temperature and low frequency. It's possible that at high temperature and low frequency the performance of the inner structural nonuniformity and instability of test specimens of **Set 4** after incomplete drying and moisture conditioning is much more evident, resulting in erroneous  $E^*$  values. Another thing that should be noted is that the same dummy sample was utilized for checking temperature for all four sets. Arguably, the presence of incompletely dried aggregates and moisture during moisture conditioning can alter the thermal properties of the samples, and the temperature in samples from the four different sets, after the same amount of time of conditioning (as predicted by the dummy sample, which was from a completely dry aggregate without moisture conditioning) could be significantly different. This difference in temperature obviously would have a significant effect on the  $E^*$  and the phase angle values.

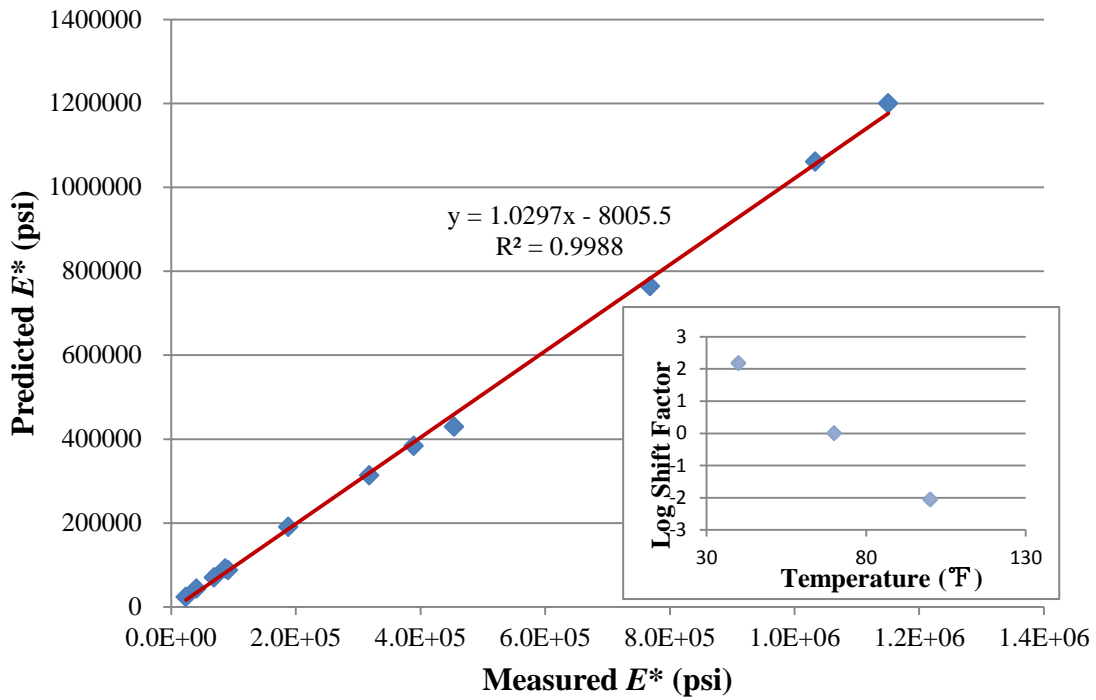


Figure 26. Predicted  $E^*$  vs. Measured  $E^*$  of Set 1

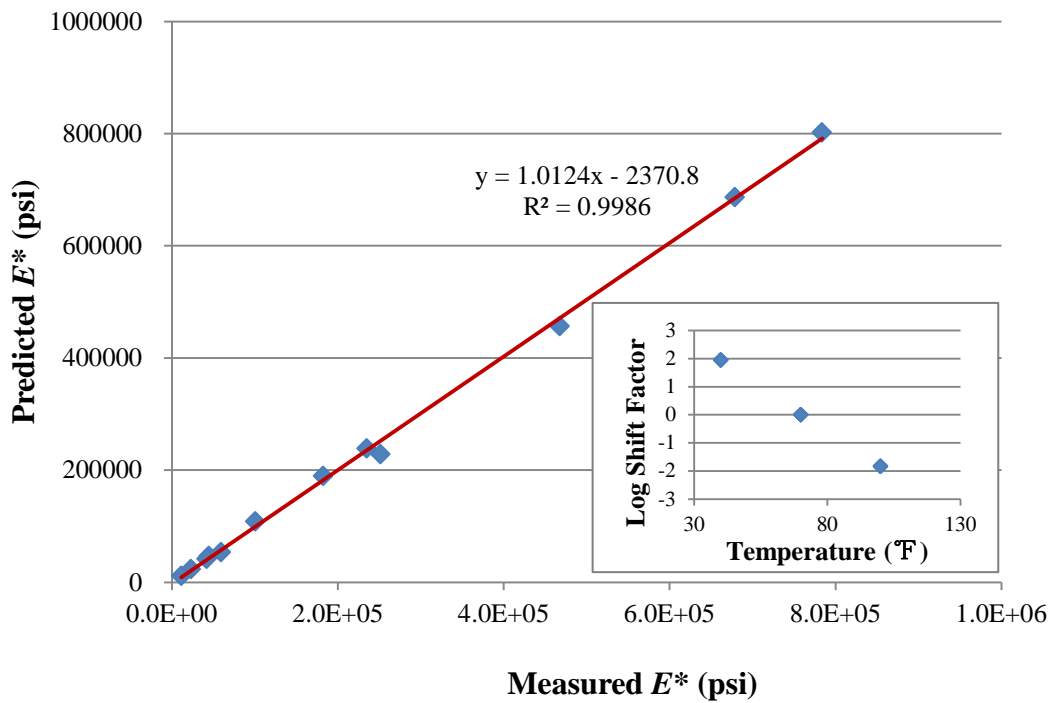


Figure 27. Predicted  $E^*$  vs. Measured  $E^*$  of Set 2

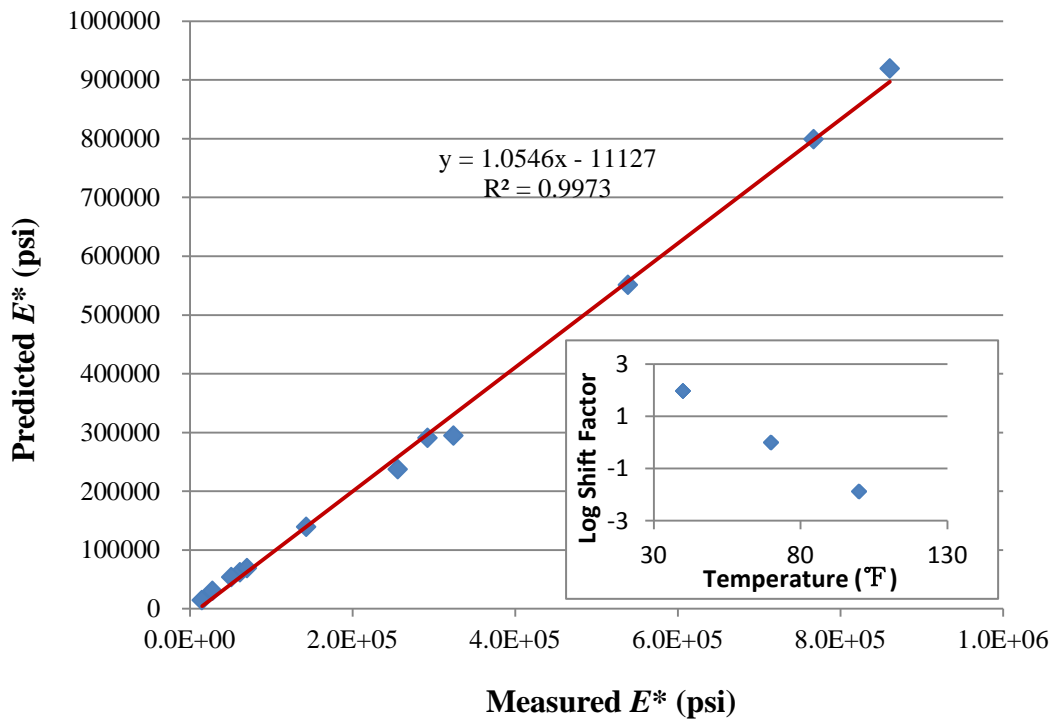


Figure 28. Predicted  $E^*$  vs. Measured  $E^*$  of Set 3

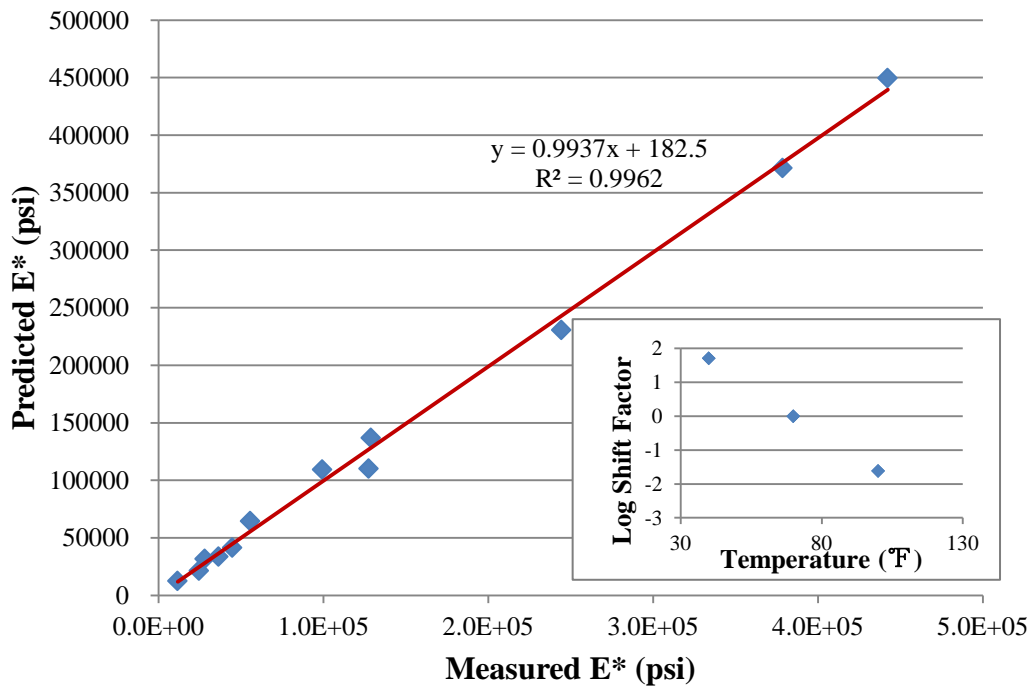
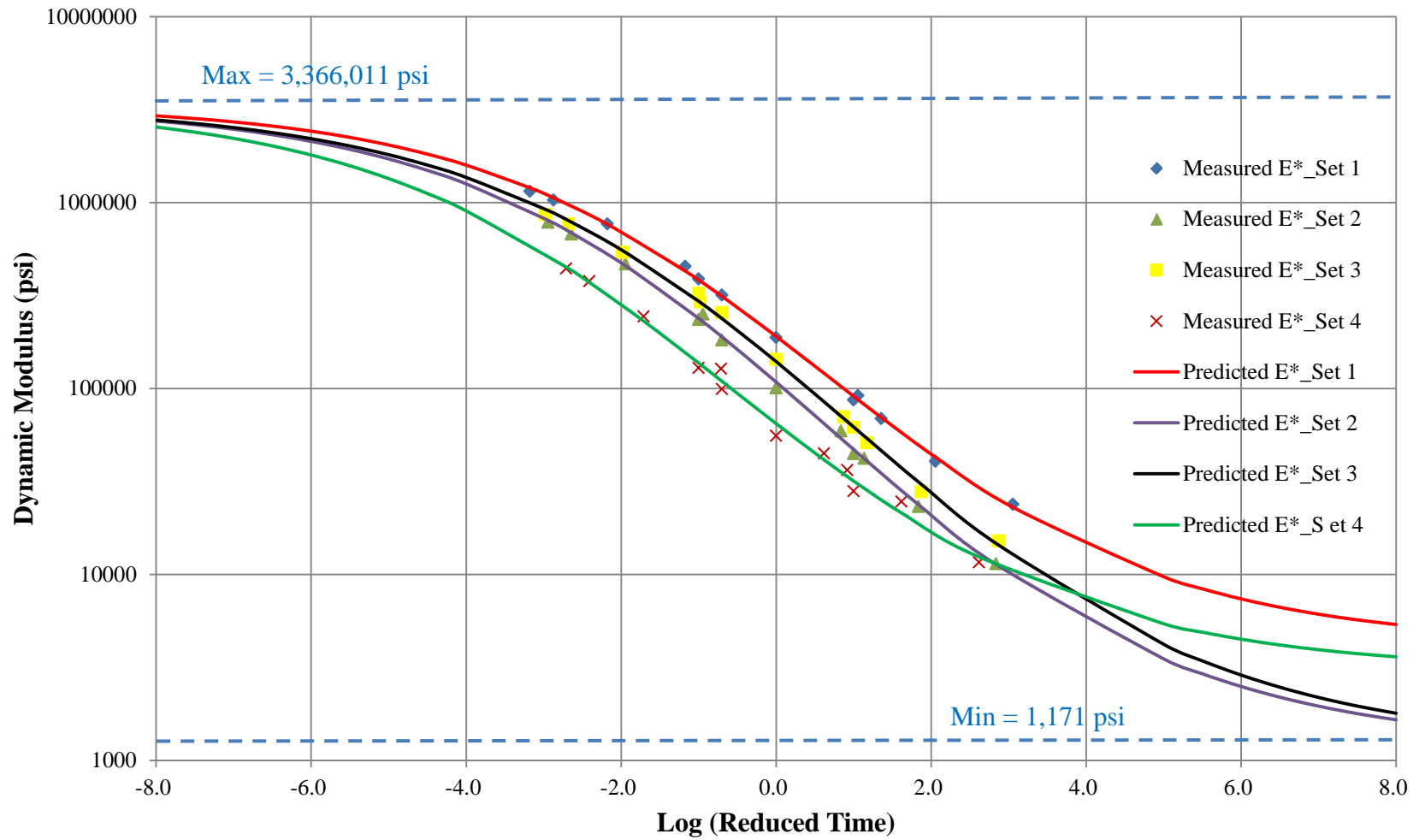


Figure 29. Predicted  $E^*$  vs. Measured  $E^*$  of Set 4



**Figure 30. Dynamic Modulus Mater Curve of Four-set Mixtures**

## 4.4 MEPDG Analysis

### 4.4.1 Inputs and Analysis

The scope of MEPDG analysis involved the collection of reliable data, selecting accurate models and simulating the field performance within the design life. The objective of this work was not to determine whether these designs were good or bad, but to compare the responses for mixes with and without moisture conditioned aggregates. There were two ways to obtain data in terms of predictive levels required. For the part of asphalt mix property, Level 1 was selected since data from laboratory test or Maine DOT database like dynamic modulus of asphalt mixture and shear modulus of asphalt binder were already procured, which enable us to increase the accuracy of the prediction. However, Level 3 was selected for other factors due to lack of regional or site-specific information and in some cases default values and assumptions, like vehicle class and hourly truck distribution, were employed instead of large amounts of field investigations.

The model of a new flexible pavement with a design life of 15 years was created, which consisted of three layers above the subgrade – 5 inch of WMA over 8 inch of cold recycled RAP base over 18 inch of crushed gravel subbase [25]. An A-2-4 soil was used for subgrade modeling based on the soil condition of Maine. Assuming a good quality of construction, an initial International Roughness Index (IRI) of 63 in/mi was used for design purposes [21]. For traffic inputs, the initial two-way AADTT of 345 was selected in consideration of the design of a low traffic pavement. In design direction, two lanes and 40% of trucks were assumed with an operational speed of 40 mph. Only default values recommended from MEPDG can be used for other traffic parameters such as traffic volume adjustment factors and axle load distribution factors due to lack of information of Maine DOT database. Besides the effect of traffic, the climatic factor is also a significant point for simulating the pavement performance. With the aid of Enhanced Integrated Climatic Model (EICM) incorporated in Design Guide, the weather station of Portland, ME was used to establish the climatic model. The depth of the water table was designed as 15 feet at this site.

With respect to the structure design, three layers with various materials above subgrade were considered for all four mixture sets with the purpose of consistency and reliability. The MEPDG software version 1.100 provides two regression models that predict  $E^*$  from more commonly available mixture parameters before setting the design layers. The “NCHRP 1-37A” viscosity based model rather than the “NCHRP 1-40D” model based on  $G^*$  values was finally used since the first approach has been nationally calibrated. As the most important design part, asphalt material properties were required to choose Level 1

based on the direct inputs of  $E^*$  values and phase angles generated from dynamic modulus tests as well as  $G^*$  values back calculated using Hirsch model. Since  $G^*$  reflects the properties of asphalt binder, only predicted  $E^*$  values of Set 1, which was prepared with fully dried aggregates and without being moisture conditioned, was considered to perform back calculation.  $E^*$  values at 10 Hz at three different temperatures (4.4 21.1 37.8°C) were used based on the requirement of MEPDG. MatLAB code for back calculation can be found in Appendix D. Table 7 summarizes the  $G^*$  values corresponding to each temperature at 10 Hz. In this part, two parameters regarding thermal properties are the thermal conductivity and heat capacity asphalt, which are regardless of input level. The default values were used since no relevant tests were conducted.

**Table 7. Back Calculating  $G^*$  at 10 Hz**

Temperature (°F)	$G^*$ (Pa)
40	2710
70	219
100	13

The properties of base, subbase and subgrade were summarized in Table 8. Note that Level 3 was used for all these three layers by reason that Level 1 inputs utilize the stress dependent FEM which has not been calibrated with distress. Due to lack of site-specific information, the default values were employed for the part of Independence Construction Materials (ICM). For the last part of design, Level 3 was used for the thermal cracking part, where average tensile strength and creep compliance at different temperatures and loading times can be automatically calculated by MEPDG software. However, thermal cracking was not evaluated in this study.

**Table 8. Properties of Asphalt Pavement Layers**

Type of Layers	Type of Materials	Input Level	Thickness (in.)	Poisson's Ratio	Modulus (psi)
Surface	Warm Mix Asphalt	1	5	-	-
Base	Cold Recycled Asphalt - RAP (includes milling)	3	8	0.35	40,000
Subbase	Crushed gravel	3	18	0.35	30,000
Subgrade	A-2-4	3	Semi-infinite	0.40	25,000

#### 4.4.2 Results of Analysis

The output summary, in the form of a spreadsheet, generated by MEPDG software provided all kinds of major distress data and plots for each month over the entire design life of 15 years. Note that only the results of bottom-up fatigue cracking (alligator cracking) and rutting were analyzed in this study, considering the presence or absence of moisture which can most likely affect the occurrence of these distresses. The analysis of thermal cracking from MEPDG simulations wasn't included in this study because prediction of thermal cracking requires not only  $E^*$  values, but other parameters such as creep compliance, and the variation in  $E^*$  alone is not sufficient to justify any comparison in that aspect.

##### *Fatigue Cracking (Alligator Cracking)*

Alligator cracking is a type of fatigue cracking which happens when a pavement is subjected to repeated tensile stress/strain at the bottom of the asphalt layer resulting in a chicken wire/alligator pattern. It is usually found on wheel paths and starts from the bottom and moves upward [26]. The results of four sets of the alligator cracking are summarized in Table 9. Also Figure 31 illustrates the propagation trend of the predicted alligator cracking by month during the whole design life.

**Table 9. Predicted Alligator Cracking and Years to Failure**

Set ID	Maximum Cracking, 15 Years (%)	Years to Failure, (25%)
Set 1	5.85	> 30 Years
Set 2	9.15	> 30 Years
Set 3	7.99	> 30 Years
Set 4	12.3	25.7

Apparently, alligator cracking was observed to be insignificant for any test set according to the critical value of 25% over the design life of 15 years. Even for the worst set concluded from dynamic modulus tests, **Set 4** tends to be fail in 25.7 years, while the other sets possess the resistance of alligator cracking after 30 years' service. As expected, the linear increment of **Set 4** fatigue cracking is obviously higher than those of other sets (Figure 31). The results verify that the presence of moisture and the process of moisture conditioning do differentiate the field performance of each set, but these pavements prepared with four kinds of mixtures can be sufficiently resistant to alligator cracking. As discussed previously,  $|E^*| \sin \delta$  at the temperature of 21.1°C is associated with fatigue resistance of pavements and Figure 22 also plots the results of four sets by frequencies. The decreasing trend of the results from the highest frequency to the lowest one as well



as abiding by the sequence of **Set 1**, **Set 3**, **Set 2** and **Set 4** can be found clearly from that figure, which completely agrees with the propagation trend of the alligator cracking predicted from MEPDG.

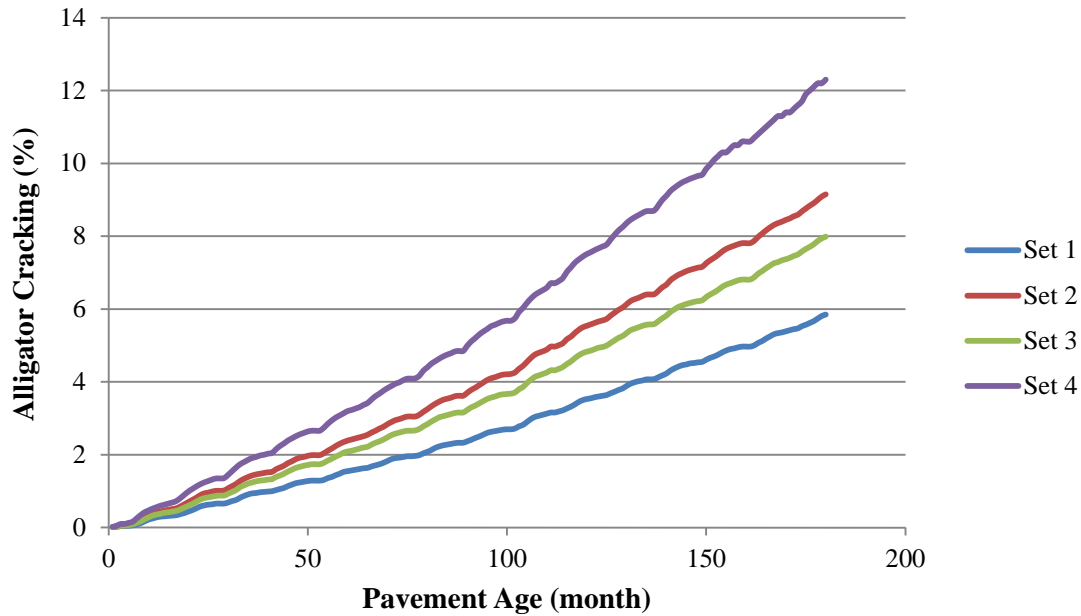


**Figure 31. Propagation Trend of the Alligator Cracking**

***Rutting***

Rutting is a kind of longitudinal depression in the wheel path, with or without transverse displacement resulting from repeated loading associated with high temperature and/or poor mix [16, 26]. It can occur in any pavement layer including subgrade, but surface ruts occur because of failure in asphalt mixes. The results of rutting for asphalt concrete mix only and the entire pavement are presented in Table 10 and Table 11, respectively. Also Figure 32 and 33 illustrate the propagation trend of the predicted rutting by month during the whole design life.

**Table 10. Rutting Depth of the Asphalt Concrete Layer and Years to Failure**

Set ID	Rutting Depth, 15 Years, (inches)	Years to Failure, (0.25 inch)
Set 1	0.1332	> 30 Years
Set 2	0.2121	21.8
Set 3	0.1724	> 30 Years
Set 4	0.3463	6.83

**Table 11. Rutting Depth of the Entire Pavement and Years to Failure**

Set ID	Rutting Depth, 15 Years, (inches)	Years to Failure, (0.75 inch)
Set 1	0.3992	> 30 Years
Set 2	0.4996	> 30 Years
Set 3	0.4524	> 30 Years
Set 4	0.6615	21.8

It is clear that the asphalt mix layers constructed with mixtures of **Set 1** and **Set 3** were adequately strong to resist against rutting significantly. As anticipated, **Set 2** and **Set 4** were much weaker compared to other sets that were without moisture conditioning. For the weakest mixture of **Set 4** it took only 6.83 years to fail in terms of the design limit of 0.25 inch. Again, with respect to the entire pavement, MEPDG software predicted the ability of resisting rutting of four mixtures as per the following sequence: **Set 1**> **Set 3**> **Set 2**> **Set 4**. From rutting figures of both the asphalt concrete layers and the total pavement, it also can be seen that the propagation of rutting in **Set 4** and **Set 2** with moisture conditioning was much faster than that of **Set 3** and **Set 1** by month. It well demonstrated that incompletely dried aggregates and moisture conditionings were able to remarkably diminish the resistance of asphalt pavements against rutting, which followed the same trend obtained in the dynamic modulus results. Note that the fact that more rutting depth can be found in **Set 2** with moisture conditioning than **Set 3** with incompletely dried aggregates means that moisture conditioning has more negative effects on asphalt mixture properties and field performance.

Again, in the part of analysis of dynamic modulus results,  $|E^*|/\sin\delta$  at the temperature of 54.4°C is associated with rutting resistance of pavements and Figure 21 also plots the results of four sets by frequencies. Relatively, the results of MEPDG prediction reflects the trend of  $|E^*|/\sin\delta$ , which means **Set 1** has the strongest property while **Set 4** has the weakest.

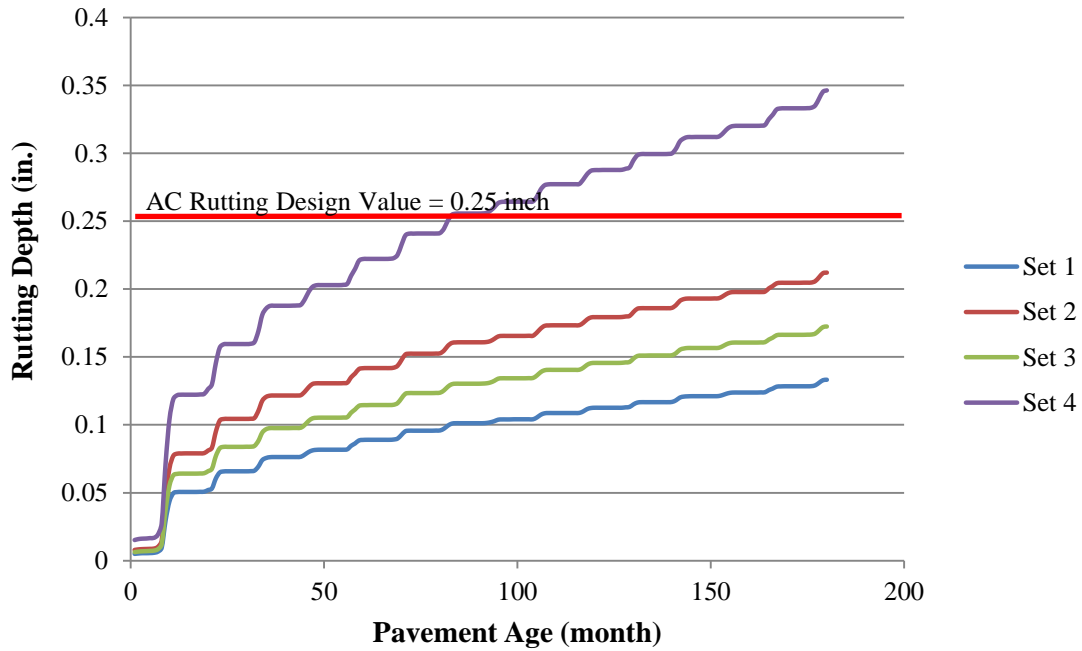


**Figure 32. Propagation Trend of Rutting of Asphalt Concrete Layer**

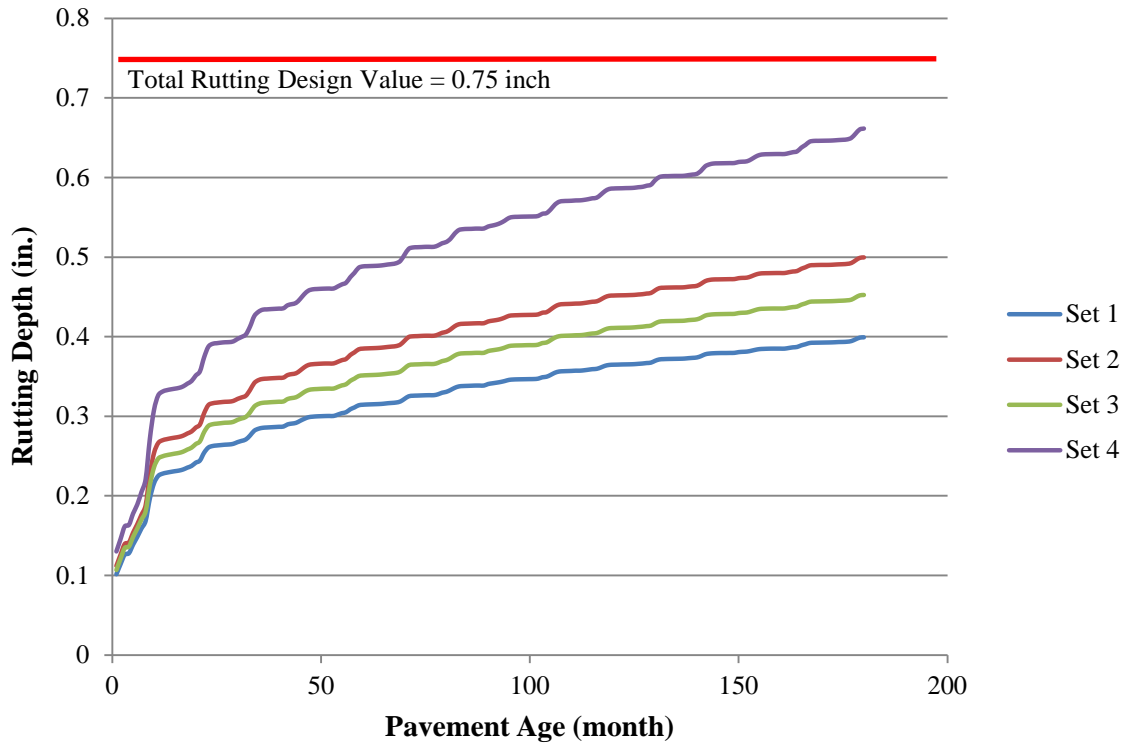


**Figure 33. Propagation Trend of Rutting of Entire Pavement**

## 5. Conclusions

The goal of this study is to investigate effects of moisture susceptibility of warm mix asphalt (WMA) mixes on dynamic modulus and field performance. The primary conclusions from the test results and analysis are as follows:

1. For producing incompletely dried aggregates, controlling moisture content within 0.5% is essential to guarantee good aggregate coating and also keep enough residual moisture in the aggregates.
2. Incompletely dried aggregates had no significant influence on VTM of test specimens compared with completely dried aggregates.
3. Moisture can negatively influence the dynamic modulus values and moisture conditioning had more effect than incomplete dry.
4. Phase angle cannot be measured correctly at high temperature with high frequency, since the glued gage points, especially attached to the matrix of fine aggregates with moisture conditioning, may loosen in such condition.
5. The dynamic modulus results of four sets were found to be significantly different, except the values at the lowest frequency at 21.1 and 37.8°C.
6. Hirsch model is effective in predicting accurate and reliable  $E^*$  values from measured values.
7. The presence of moisture can cause significant effect on alligator cracking, but all mixtures can be sufficiently resistant to this distress during the design life.
8. Moisture conditioning was able to more remarkably diminish the resistance of asphalt pavements against rutting than those prepared with incompletely drying of aggregates.

## 6. Recommendations

With respect to the dynamic modulus tests and MEPDG simulation, the following recommendations are suggested:

1. The dummy sample in the environment chamber used for measuring temperatures is recommended to be with the same properties as the test specimens.
2. A more effective and reliable approach to control moisture contents of incompletely dried aggregates within a small variation range to guarantee consistency of each test specimen should be investigated further.
3. The use of more secure gages attached to the surface of specimens is highly recommended to avoid loosening in the case of high temperature and high frequency during the dynamic modulus tests.
4. The use of Hirsch model is recommended for conducting the master curve compared with other predictive models.
5. Mixes prepared at low temperatures, such as in WMA, should be properly tested and designed to resist the effect of moisture conditioning/distress during field performance.

## References

1. Bhusal, S., *A Laboratory Study of Warm Mix Asphalt for Moisture Damage Potential And Performances Issues*. December, 2008, Oklahoma State University.
2. Lee, H.D. and Y.T. Kim, *Performance Measures of Warm Asphalt Mixtures for Safe and Reliable Freight Transportation*. April 2009, Public Policy Center, University of Iowa.
3. Mallick, R.B., et al., *A Practical Method to Understand the Effect of Aggregate Drying on the Moisture Content of Hot Mix Asphalt (HMA)*, in *The 90th Annual Meeting of the Transportation Research Board*. January 2011: Washington, DC.
4. Gong, W., *Investigation of Moisture Susceptibility of Warm Mix Asphalt (WMA) Mixes through Laboratory Mechanical Testing*. June 2011, Worcester Polytechnic Institute: Worcester, MA.
5. Witczak, M.W., et al., *Simple Performance Test for Superpave Mix Design*, *NCHRP, Report 465*. 2002.
6. Solaimanian, M., R.F. Bonaquist, and V. Tandon, *NCHRP Report 589: Improved Conditioning and Testing Procedures for HMA Moisture Susceptibility*. 2007, Transportation Research Board: Washington, D.C.
7. Bonaquist, R., *NCHRP Report 614: Refining the Simple Performance Tester for Use in Routine Practice*. 2008, Transportation Research Board: Washington, D.C.
8. Ali, O., *Evaluation of the Mechanistic Empirical Pavement Design Guide (NCHRP 1-37 A)*. September 2005.
9. Dzotepe, G. and K. Ksaibati, *Implementation of the Mechanistic-Empirical Pavement Design Guide (MEPDG)*. September 2010, Department of Civil and Architectural Engineering, University of Wyoming: Laramie, WY.
10. Hossain, Z., et al., *Evaluation of the Use of Warm Mix Asphalt as a Viable Paving Material in the United States*. November 2009, Federal Highway Administration.
11. Bonaquist, R., *NCHRP Report 691: Mix Design Practices for Warm Mix Asphalt*. 2011, Transportation Research Board: Washington D.C.
12. Bonaquist, R., *Mix Design Practices for Warm Mix Asphalt, NCHRP 9-43, Interim Report*. 2008, National Cooperation Highway Research Program: Washington D.C.
13. Kantipong, K.S., et al., *Laboratory Study on Warm Mix Asphalt Additives*, in *TRB 2007 Annual Meeting*. 2007: Washington, D.C.
14. Goh, S.W., Y. Liu, and Z. You, *Laboratory Evaluation of Warm Mix Asphalt Using Sasobit®*, in *Bearing Capacity of Roads, Railways and Airfields. 8th International Conference (BCR2A'09)*. 2009: Champaign IL. p. 315-320.
15. Corrigan, M., D. Newcomb, and T. Bennert, *From Hot to Warm*. Public Roads, 2010(July/August 2010): p. 23-29.

16. Tashman, L. and M.A. Elangovan, *Dynamic Modulus Test - Laboratory Investigation and Future Implementation in the State Of Washington*. December 2007, Washington State Transportation Center (TRAC), University of Washington.
17. Dougan, C.E., et al., *E\* - Dynamic Modulus Test Protocol – Problems and Solutions*. March 2003, University of Connecticut, Connecticut Transportation Institute.
18. Zhou, F. and T. Scullion, *Case Study: Preliminary Field Validation of Simple Performance Tests for Permanent Deformation*, in *The 82th Annual Meeting of the Transportation Research Board*. 2003: Washington, DC.
19. You, Z., S.W. Goh, and R.C. Williams, *Development of Specification for the Superpave Simple Performance Tests (SPT)*. May 2009, Department of Civil and Environmental Engineering, Michigan Technological University.
20. *AASHTO TP 62-03*, in *Standard Method of Test for Determining Dynamic Modulus of Hot-Mix Asphalt Concrete Mixtures* 2005, American Association of State and Highway Transportation Officials.
21. *Guide for Mechanistic-Empirical Design of New and Rehabilitated Pavement Structures*. March 2004, National Cooperative Highway Research Program, Transportation Research Board, National Research Council Champaign, Illinois.
22. Timm, D.H., R.E. Turochy, and K.P. Davis, *Guidance for M-E Pavement Design Implementation*. January 8, 2010, Harbert Engineering Center: Auburn, Alabama.
23. O’Sullivan, K.A., *Rejuvenation of Reclaimed Asphalt Pavement (RAP) in Hot Mix Asphalt Recycling with High RAP Content*. April 2011, Worcester Polytechnic Institute: Worcester, MA.
24. Flinstch, G.W., et al., *Asphalt Materials Characterization in Support of Implementation of the Proposed Mechanistic-Empirical Pavement Design Guide*. 2007, Virginia Department of Transportation.
25. Mallick, R.B., S. Fowler, and B. Marquis, *Use of Mechanistic Empirical Pavement Design Software for Proper Design and Construction of Reclaimed Pavements*, Worcester Polytechnic Institute, Maine Department of Transportation.
26. Mallick, R.B. and T. El-Korchi, *Pavement Engineering: Principles and Practice*. 2009: New York: Taylor & Francis Group.

## Appendix A: Control of Incomplete Dry

**Table 12. The Change of the Aggregate Mass and Moisture Contents of Set 3**

Batch ID	Hours	0	0.5	1	1.5	2	2.5	3	3.5	4	4.5
1	Aggregates Weight (g) Percentage of Moisture Contents Left	7855	7755	7631	7499	7360	7223	7105	7039	7009	-
		12.57%	11.13%	9.36%	7.47%	5.47%	3.51%	1.82%	0.87%	0.44%	-
2		7969	7876	7787	7669	7550	7444	7328	7229	7109	7005
		14.20%	12.87%	11.59%	9.90%	8.20%	6.68%	5.02%	3.60%	1.88%	0.39%
3		7928	7856	7758	7653	7541	7408	7279	7173	7058	7000
		13.58%	12.55%	11.15%	9.64%	8.04%	6.13%	4.28%	2.77%	1.12%	0.29%
4		7928	7813	7676	7528	7373	7234	7079	7028	7006	-
		13.60%	11.95%	9.99%	7.87%	5.65%	3.65%	1.43%	0.70%	0.39%	-



**Table 13. The Change of the Aggregate Mass and Moisture Contents of Set 4**

Batch ID	Hours	0	0.5	1	1.5	2	2.5	3	3.5	4	4.5
1	Aggregates Weight (g) Percentage of Moisture Contents Left	7935	7875	7741	7600	7445	7323	7192	7075	7003	-
		13.80%	12.94%	11.01%	8.99%	6.77%	5.02%	3.14%	1.46%	0.43%	-
2		7870	7836	7749	7625	7526	7409	7301	7194	7066	7011
		12.82%	12.33%	11.08%	9.30%	7.88%	6.21%	4.66%	3.13%	1.29%	0.50%
3		7844	7788	7651	7512	7375	7252	7132	7036	7008	-
		12.46%	11.66%	9.69%	7.70%	5.73%	3.97%	2.25%	0.87%	0.47%	-
4		7889	7853	7760	7653	7537	7426	7318	7224	7107	7009
		13.09%	12.57%	11.24%	9.70%	8.04%	6.45%	4.90%	3.56%	1.88%	0.47%

## Appendix B: Volumetric Properties

**Table 14. The Data Analysis of Theoretical Maximum Specific Gravity ( $G_{mm}$ )**

Sample ID	Bag Weight <b>A</b>	Weight of Sample in Air <b>B</b>	Weight of Bags and Samples in Water <b>C</b>	Total Volume <b>D = A + B - C</b>	Bag Volume <b>E = A/V<sub>c</sub></b>	Sample Volume <b>F = D - E</b>	TMD <b>G = B/F</b>	Average	Standard Deviation
1	74.7	2026.8	1174.8	926.7	82.724	843.976	2.401	2.398	0.00921
2	74.9	2035.8	1181.4	929.3	82.946	846.354	2.405		
3	75.9	2017.6	1164.5	929.0	84.053	844.947	2.388		

**Note:** Herein, the correction factor  $V_c$  has been given as  $0.903 \text{ g/cm}^3$  according to CoreLok manual.

**Table 15. The Data Analysis of Bulk Specific Gravity and Air Voids of Set 1**

Sample ID	A Bag Weight (g)	B Dry Sample Weight before Sealing (g)	C Sealed Sample Weight in Water (g)	D Dry Sample Weight after Water Submersion (g)	E Ratio B / A	F Bag Volume Correction from Table	G Total Volume (A + D) - C	H Volume of Bag A / F	I Volume of Sample G - H	J Bulk Specific Gravity B / I	K Theoretical Maximum Specific Gravity	L Air Voids
1A	76.6	2602.2	1404.3	2601.5	34.0	0.739	1273.8	103.7	1170.1	2.224	2.398	7.26%
1B	76.4	2601.1	1407.4	2599.8	34.0	0.739	1268.8	103.4	1165.4	2.232	2.398	6.92%
1C	76.5	2601.4	1408.7	2600.3	34.0	0.739	1268.1	103.5	1164.6	2.234	2.398	6.85%
1D	76.1	2597.6	1402.3	2596.4	34.1	0.739	1270.2	103.0	1167.2	2.226	2.398	7.19%

*Note: Herein, the correction factors of Table 15 to 18 were calculated by the equation of  $-0.0022448 * \text{Ratio} + 0.81518$  according to CoreLok manual (the same hereinafter).*

**Table 16. The Data Analysis of Bulk Specific Gravity and Air Voids of Set 2**

Sample ID	A Bag Weight (g)	B Dry Sample Weight before Sealing (g)	C Sealed Sample Weight in Water (g)	D Dry Sample Weight after Water Submersion (g)	E Ratio B / A	F Bag Volume Correction from Table	G Total Volume (A + D) - C	H Volume of Bag A / F	I Volume of Sample G - H	J Bulk Specific Gravity B / I	K Theoretical Maximum Specific Gravity	L Air Voids
2A	75.5	2595.3	1397.1	2593.7	34.4	0.738	1272.1	102.3	1169.8	2.219	2.398	7.48%
2B	74.9	2607.3	1409.3	2605.7	34.8	0.737	1271.3	101.6	1169.7	2.229	2.398	7.04%
2C	75.5	2599.1	1402.8	2597.5	34.4	0.738	1270.2	102.3	1167.9	2.225	2.398	7.19%
2D	74.6	2608.9	1413.9	2607.3	35.0	0.737	1268.0	101.3	1166.7	2.236	2.398	6.75%

**Table 17. The Data Analysis of Bulk Specific Gravity and Air Voids of Set 3**

Sample ID	A Bag Weight (g)	B Dry Sample Weight before Sealing (g)	C Sealed Sample Weight in Water (g)	D Dry Sample Weight after Water Submersion (g)	E Ratio B / A	F Bag Volume Correction from Table	G Total Volume (A + D) - C	H Volume of Bag A / F	I Volume of Sample G - H	J Bulk Specific Gravity B / I	K Theoretical Maximum Specific Gravity	L Air Voids
3A	75.5	2603.7	1406.6	2602.4	34.5	0.738	1271.3	102.3	1169.0	2.227	2.398	7.12%
3B	75.3	2598.4	1404.1	2597.7	34.5	0.738	1268.9	102.1	1166.8	2.227	2.398	7.14%
3C	75.5	2597.4	1396.5	2595.8	34.4	0.738	1274.8	102.3	1172.5	2.215	2.398	7.62%
3D	75.2	2611.5	1418.4	2610.6	34.7	0.737	1267.4	102.0	1165.4	2.241	2.398	6.55%

**Table 18. The Data Analysis of Bulk Specific Gravity and Air Voids of Set 4**

Sample ID	A Bag Weight (g)	B Dry Sample Weight before Sealing (g)	C Sealed Sample Weight in Water (g)	D Dry Sample Weight after Water Submersion (g)	E Ratio B / A	F Bag Volume Correction from Table	G Total Volume (A + D) - C	H Volume of Bag A / F	I Volume of Sample G - H	J Bulk Specific Gravity B / I	K Theoretical Maximum Specific Gravity	L Air Voids
4A	74.9	2604.5	1408.1	2602.9	34.8	0.737	1269.7	101.6	1168.1	2.230	2.398	7.02%
4B	74.8	2590.4	1399.7	2589.1	34.6	0.737	1264.2	101.4	1162.8	2.228	2.398	7.10%
4C	74.9	2603.7	1411.5	2602.3	34.8	0.737	1265.7	101.6	1164.1	2.237	2.398	6.73%
4D	74.9	2606.8	1413.7	2605.4	34.8	0.737	1266.6	101.6	1165.0	2.238	2.398	6.69%

**Table 19. The Average and Standard Deviation of VTM**

Mix ID	Sample ID	VTM	Average	Difference	Standard Deviation
Set 1	1A	7.62%	7.06%	0.56%	0.00202
	1B	6.92%		-0.14%	
	1C	6.85%		-0.21%	
	1D	7.19%		0.13%	
Set 2	2A	7.48%	7.12%	0.36%	0.00304
	2B	7.04%		-0.08%	
	2C	7.19%		0.07%	
	2D	6.75%		-0.37%	
Set 3	3A	7.12%	7.11%	0.01%	0.00436
	3B	7.14%		0.03%	
	3C	7.62%		0.51%	
	3D	6.55%		-0.56%	
Set 4	4A	7.02%	6.88%	0.14%	0.00206
	4B	7.10%		0.22%	
	4C	6.73%		-0.15%	
	4D	6.69%		-0.19%	

## Appendix C: Dynamic Modulus Test and Master Curve

Table 20. The Average of Dynamic Modulus and Phase Angle Results

Temperature (°C (°F))	Frequency (Hz)	Set 1		Set 2		Set 3		Set 4	
		Dynamic Modulus (psi)	Phase Angle (°)	Dynamic Modulus (psi)	Phase Angle (°)	Dynamic Modulus (psi)	Phase Angle (°)	Dynamic Modulus (psi)	Phase Angle (°)
4.4 (40)	10	1150333	15.276	783890	19.714	860833	18.100	442240	25.294
	5	1033087	15.829	678683	20.252	767320	18.847	378497	25.652
	1	767997	18.836	467820	23.569	538937	22.612	244413	28.008
	0.1	453895	25.487	251640	28.446	292670	29.721	127563	30.349
21.1 (70)	10	389150	27.237	235140	38.799	324177	29.414	128940	37.008
	5	317810	27.839	182347	31.445	255883	30.360	99248	32.430
	1	187983	30.744	100650	33.035	143313	32.847	55652	31.412
	0.1	86661	31.322	44663	31.364	61778	32.630	28058	27.297
37.8 (100)	10	91594	49.373	59237	3.518	70366	5.220	44761	3.375
	5	68957	29.622	42200	34.749	51203	35.485	36380	31.747
	1	40570	26.362	23239	31.689	27911	32.341	24667	26.305
	0.1	23823	20.648	11432	24.408	15120	24.867	11622	23.398
54.4 (130)	10	40814	5.232	16519	9.920	26132	8.722	13559	9.635
	5	30047	28.526	15081	25.896	38684	35.489	14285	25.633
	1	20790	24.767	9695	21.920	24192	17.935	7564	23.177
	0.1	15009	18.064	9977	14.372	9207	23.979	5927	19.032



**Table 21.  $|E^*|/\sin\delta$  and  $|E^*|\sin\delta$  Results**

Temperature (°C (°F))	Frequency (Hz)	Set 1		Set 2		Set 3		Set 4	
		$ E^* /\sin\delta$	$ E^* \sin\delta$	$ E^* /\sin\delta$	$ E^* \sin\delta$	$ E^* /\sin\delta$	$ E^* \sin\delta$	$ E^* /\sin\delta$	$ E^* \sin\delta$
4.4 (40)	10	4366104	303077	2323840	264426	2770835	267441	1035040	188955
	5	3787431	281792	1960663	234926	2375294	247877	874320	163853
	1	2378728	247956	1169979	187059	1401698	207215	520471	114776
	0.1	1054818	195314	528289	119864	590326	145099	252465	64454
21.1 (70)	10	850281	178103	375269	147336	660082	159209	214211	77613
	5	680552	148414	349538	95127	506266	129331	185071	53223
	1	367727	96097	184628	54869	264221	77733	106777	29005
	0.1	166705	45050	85812	23246	114571	33311	61183	12867
37.8 (100)	10	120683	69517	965368	3635	773421	6402	760332	2635
	5	139511	34084	74037	24053	88207	29723	69141	19142
	1	91365	18015	44239	12208	52174	14931	55663	10931
	0.1	67559	8401	27665	4724	35956	6358	29266	4615
54.4 (130)	10	447577	3722	95889	2846	172329	3963	81010	2269
	5	62918	14349	34531	6586	66634	22458	33020	6180
	1	49627	8710	25970	3619	78561	7450	19218	2977
	0.1	48404	4654	40195	2476	22655	3742	18176	1933

**Table 22. Std./Ave. of  $E^*$  Results of Set 1**

Temperature (°C (°F))	Frequency (Hz)	Ave. of $E^*$	Std. of $E^*$	Std./Ave. of $E^*$
4.4 (40)	10	1150333	110988	9.65%
	5	1033087	92587	8.96%
	1	767997	63919	8.32%
	0.1	453895	35965	7.92%
21.1 (70)	10	389150	46071	11.84%
	5	317810	37958	11.94%
	1	187983	23887	12.71%
	0.1	86661	8432	9.73%
37.8 (100)	10	91594	7822	8.54%
	5	68957	5663	8.21%
	1	40570	3558	8.77%
	0.1	23823	2436	10.23%
54.4 (130)	10	40814	20663	50.63%
	5	30047	15189	50.55%
	1	20790	3681	17.71%
	0.1	15009	6887	45.89%

**Table 23. Std./Ave. of  $E^*$  Results of Set 2**

Temperature (°C (°F))	Frequency (Hz)	Ave. of $E^*$	Std. of $E^*$	Std./Ave. of $E^*$
4.4 (40)	10	783890	139704	17.82%
	5	678683	145590	21.45%
	1	467820	126472	27.03%
	0.1	251640	82538	32.80%
21.1 (70)	10	235140	54527	23.19%
	5	182347	44448	24.38%
	1	100650	24835	24.67%
	0.1	44663	9442	21.14%
37.8 (100)	10	59237	11463	19.35%
	5	42200	7574	17.95%
	1	23239	3504	15.08%
	0.1	11432	823	7.20%
54.4 (130)	10	16519	2328	14.09%
	5	15081	4818	31.95%
	1	9695	1235	12.74%
	0.1	9977	7690	77.07%

**Table 24. Std./Ave. of  $E^*$  Results of Set 3**


Temperature (°C (°F))	Frequency (Hz)	Ave. of $E^*$	Std. of $E^*$	Std./Ave. of $E^*$
4.4 (40)	10	860833	4832	0.56%
	5	767320	5515	0.72%
	1	538937	8159	1.51%
	0.1	292670	8158	2.79%
21.1 (70)	10	324177	28481	8.79%
	5	255883	21354	8.35%
	1	143313	11836	8.26%
	0.1	61778	4452	7.21%
37.8 (100)	10	70366	5856	8.32%
	5	51203	3653	7.13%
	1	27911	2555	9.15%
	0.1	15120	2826	18.69%
54.4 (130)	10	26132	1802	6.89%
	5	38684	25344	65.51%
	1	24192	18187	75.18%
	0.1	9207	947	10.28%

**Table 25. Std./Ave. of  $E^*$  Results of Set 4**

Temperature (°C (°F))	Frequency (Hz)	Ave. of $E^*$	Std. of $E^*$	Std./Ave. of $E^*$
4.4 (40)	10	442240	11634	2.63%
	5	378497	18880	4.99%
	1	244413	20025	8.19%
	0.1	127563	15397	12.07%
21.1 (70)	10	128940	21453	16.64%
	5	99248	18275	18.41%
	1	55652	9480	17.04%
	0.1	28058	4421	15.76%
37.8 (100)	10	44761	5105	11.40%
	5	36380	7671	21.09%
	1	24667	4350	17.63%
	0.1	11622	2298	19.77%
54.4 (130)	10	13559	4123	30.41%
	5	14285	5058	35.41%
	1	7564	2260	29.88%
	0.1	5927	2319	39.13%


**Table 26. Computational Process of Master Curve of Set 1**

Parameters	A	VTS	VFA	VMA	Reference Temp., (°F)	P <sub>c</sub>	E*  <sub>max</sub> , psi
	10.312	-3.440	67.17	21.49	70	0.9997313573	3359600

Temp. (°F)	Freq. (Hz)	E* (psi)	Temp. (R)	Viscosity (cP)	Log E*	$\delta$	$\beta$	$\gamma$	$c$	$t$	Log( $t$ )	Log [a(T)]	Log ( $t_r$ )	Log E <sub>predicted</sub>	Error <sup>2</sup>	E <sub>predicted</sub>			
40	10	1150333	499.67	1.93E+10	6.06082	3.63	-0.28	0.45	2.50	0.1	-1	2.17	-3.17	6.07896	3.29E-04	1199393			
40	5	1033087	499.67	1.93E+10	6.01414	 Determined by Solver				0.2	-0.699	2.17	-2.87	6.02567	1.33E-04	1060901			
40	1	767997	499.67	1.93E+10	5.88536					1	0	2.17	-2.17	5.88287	6.19E-06	763609			
40	0.1	453895	499.67	1.93E+10	5.65696					10	1	2.17	-1.17	5.63217	6.14E-04	428714			
70	10	389150	529.67	2.60E+09	5.59012					0.1	-1	0.00	-1.00	5.58321	4.77E-05	383011			
70	5	317810	529.67	2.60E+09	5.50217					0.2	-0.699	0.00	-0.70	5.49569	4.19E-05	313106			
70	1	187983	529.67	2.60E+09	5.27412					1	0	0.00	0.00	5.28024	3.75E-05	190653			
70	0.1	86661	529.67	2.60E+09	4.93782					10	1	0.00	1.00	4.95798	4.06E-04	90777			
100	10	91594	559.67	3.90E+08	4.96187					0.1	-1	-2.05	1.05	4.94037	4.62E-04	87171			
100	5	68957	559.67	3.90E+08	4.83858					0.2	-0.699	-2.05	1.36	4.84449	3.49E-05	69901			
100	1	40570	559.67	3.90E+08	4.60821					1	0	-2.05	2.05	4.63098	5.19E-04	42754			
100	0.1	23823	559.67	3.90E+08	4.37700					10	1	-2.05	3.05	4.36075	2.64E-04	22948			
														<b>Sum of Error<sup>2</sup></b>	2.90E-03				


**Table 27. Computational Process of Master Curve of Set 2**

Parameters	A	VTS	VFA	VMA	Reference Temp., °F	P <sub>c</sub>	E*  <sub>max</sub> , psi
	10.312	-3.440	66.96	21.54	70	0.9997298884	3357445

Temp. (°F)	Freq. (Hz)	E* (psi)	Temp. (R)	Viscosity (cP)	Log E*	$\delta$	$\beta$	$\gamma$	$c$	$t$	Log( $t$ )	Log [a(T)]	Log ( $t_r$ )	Log E <sub>predicted</sub>	Error <sup>2</sup>	E <sub>predicted</sub>
40	10	783890	499.67	1.93E+10	5.89426	3.07	-0.28	0.42	2.23	0.1	-1	1.94	-2.94	5.90418	9.86E-05	802016
40	5	678683	499.67	1.93E+10	5.83167	 <b>Determined by Solver</b>	0.2	-0.699	1.94	-2.64	5.83681	2.64E-05	686766			
40	1	467820	499.67	1.93E+10	5.67008		1	0	1.94	-1.94	5.65979	1.06E-04	456864			
40	0.1	251640	499.67	1.93E+10	5.40078		10	1	1.94	-0.94	5.35887	1.76E-03	228493			
70	10	235140	529.67	2.60E+09	5.37133		0.1	-1	0.00	-1.00	5.37727	3.53E-05	238379			
70	5	182347	529.67	2.60E+09	5.26090		0.2	-0.699	0.00	-0.70	5.27793	2.90E-04	189641			
70	1	100650	529.67	2.60E+09	5.00282		1	0	0.00	0.00	5.03470	1.02E-03	108318			
70	0.1	44663	529.67	2.60E+09	4.64994		10	1	0.00	1.00	4.67202	4.87E-04	46991			
100	10	59237	559.67	3.90E+08	4.77259		0.1	-1	-1.84	0.84	4.73150	1.69E-03	53889			
100	5	42200	559.67	3.90E+08	4.62531		0.2	-0.699	-1.84	1.14	4.62237	8.67E-06	41915			
100	1	23239	559.67	3.90E+08	4.36621		1	0	-1.84	1.84	4.37573	9.06E-05	23753			
100	0.1	11432	559.67	3.90E+08	4.05813		10	1	-1.84	2.84	4.05427	1.49E-05	11331			
														<b>Sum of Error<sup>2</sup></b>	5.62E-03	


**Table 28. Computational Process of Master Curve of Set 3**

Parameters	A	VTS	VFA	VMA	Reference Temp., °F	P <sub>c</sub>	E*  <sub>max</sub> , psi
	10.312	-3.440	67.00	21.53	70	0.9997301748	3357875

Temp. (°F)	Freq. (Hz)	E* (psi)	Temp. (R)	Viscosity (cP)	Log E*	$\delta$	$\beta$	$\gamma$	$c$	$t$	Log( $t$ )	Log [a(T)]	Log ( $t_r$ )	Log E <sub>predicted</sub>	Error <sup>2</sup>	E <sub>predicted</sub>
40	10	860833	499.67	1.93E+10	5.93492	3.07	-0.41	0.41	2.27	0.1	-1	1.98	-2.98	5.96366	8.26E-04	919726
40	5	767320	499.67	1.93E+10	5.88498	 <b>Determined by Solver</b>	0.2	-0.699	1.98	-2.68	5.90261	3.11E-04	799109			
40	1	538937	499.67	1.93E+10	5.73154		1	0	1.98	-1.98	5.74126	9.46E-05	551142			
40	0.1	292670	499.67	1.93E+10	5.46638		10	1	1.98	-0.98	5.46326	9.70E-06	290579			
70	10	324177	529.67	2.60E+09	5.51078		0.1	-1	0.00	-1.00	5.46927	1.72E-03	294622			
70	5	255883	529.67	2.60E+09	5.40804		0.2	-0.699	0.00	-0.70	5.37590	1.03E-03	237630			
70	1	143313	529.67	2.60E+09	5.15629		1	0	0.00	0.00	5.14480	1.32E-04	139573			
70	0.1	61778	529.67	2.60E+09	4.79083		10	1	0.00	1.00	4.79279	3.83E-06	62057			
100	10	70366	559.67	3.90E+08	4.84736		0.1	-1	-1.87	0.87	4.83876	7.40E-05	68986			
100	5	51203	559.67	3.90E+08	4.70930		0.2	-0.699	-1.87	1.17	4.73142	4.90E-04	53879			
100	1	27911	559.67	3.90E+08	4.44578		1	0	-1.87	1.87	4.48559	1.59E-03	30591			
100	0.1	15120	559.67	3.90E+08	4.17955		10	1	-1.87	2.87	4.15767	4.79E-04	14377			
														<b>Sum of Error<sup>2</sup></b>	6.76E-03	

**Table 29. Computational Process of Master Curve of Set 4**

Parameters	A	VTS	VFA	VMA	Reference Temp., °F	P <sub>c</sub>	E*  <sub>max</sub> , psi
	10.312	-3.440	67.75	21.34	70	0.9997355146	3366011

Temp. (°F)	Freq. (Hz)	E* (psi)	Temp. (R)	Viscosity (cP)	Log E*	$\delta$	$\beta$	$\gamma$	$c$	$t$	Log( $t$ )	Log [a(T)]	Log ( $t_r$ )	Log E <sub>predicted</sub>	Error <sup>2</sup>	E <sub>predicted</sub>
40	10	442240	499.67	1.93E+10	5.64566	3.48	0.26	0.43	1.96	0.1	-1	1.71	-2.71	5.65294	5.31E-05	449721
40	5	378497	499.67	1.93E+10	5.57806	 <b>Determined by Solver</b>	0.2	-0.699	1.71	-2.41	5.57011	6.32E-05	371633			
40	1	244413	499.67	1.93E+10	5.38812		1	0	1.71	-1.71	5.36290	6.36E-04	230621			
40	0.1	127563	499.67	1.93E+10	5.10573		10	1	1.71	-0.71	5.04247	4.00E-03	110274			
70	10	128940	529.67	2.60E+09	5.11039		0.1	-1	0.00	-1.00	5.13688	7.02E-04	137049			
70	5	99248	529.67	2.60E+09	4.99672		0.2	-0.699	0.00	-0.70	5.03869	1.76E-03	109319			
70	1	55652	529.67	2.60E+09	4.74548		1	0	0.00	0.00	4.81104	4.30E-03	64720			
70	0.1	28058	529.67	2.60E+09	4.44806		10	1	0.00	1.00	4.50234	2.95E-03	31793			
100	10	44761	559.67	3.90E+08	4.65090		0.1	-1	-1.62	0.62	4.61707	1.14E-03	41407			
100	5	36380	559.67	3.90E+08	4.56086		0.2	-0.699	-1.62	0.92	4.52659	1.17E-03	33619			
100	1	24667	559.67	3.90E+08	4.39211		1	0	-1.62	1.62	4.33119	3.71E-03	21438			
100	0.1	11622	559.67	3.90E+08	4.06528		10	1	-1.62	2.62	4.09433	8.44E-04	12426			
														<b>Sum of Error<sup>2</sup></b>	2.13E-02	

## Appendix D: ANOVA for Dynamic Modulus Results

Table 30. SNK Analysis of Homogeneous Subsets at 4.4°C

Variance	N	Subset						
		1	2	3	4	5	6	7
16.00	3	127563.3333						
15.00	3	244413.3333	244413.3333					
8.00	3	251640.0000	251640.0000					
12.00	3	292670.0000	292670.0000	292670.0000				
14.00	3		378496.6667	378496.6667	378496.6667			
13.00	3			442240.0000	442240.0000			
4.00	3			453894.6667	453894.6667			
7.00	3			467820.0000	467820.0000			
11.00	3				538936.6667			
6.00	3					678683.3333		
10.00	3					767320.0000	767320.0000	
3.00	3					767996.6667	767996.6667	
5.00	3					783890.0000	783890.0000	
9.00	3						860833.3333	
2.00	3							1033086.6667
1.00	3							1150333.3333
Sig.		.053	.152	.056	.093	.337	.439	.066



**Table 31. SNK Analysis of Homogeneous Subsets at 21.1°C**

Variance	N	Subset							
		1	2	3	4	5	6	7	8
16.00	3	28058.3333							
8.00	3	44662.6667	44662.6667						
15.00	3	55651.6667	55651.6667						
12.00	3	61778.0000	61778.0000						
4.00	3	86661.0000	86661.0000	86661.0000					
14.00	3		99247.6667	99247.6667					
7.00	3		100650.3333	100650.3333					
13.00	3			128940.0000	128940.0000				
11.00	3			143313.3333	143313.3333				
6.00	3				182346.6667	182346.6667			
3.00	3				187983.3333	187983.3333			
5.00	3					235140.0000	235140.0000		
10.00	3						255883.3333		
2.00	3							317810.0000	
9.00	3							324176.6667	
1.00	3								389150.0000
Sig.		.094	.159	.113	.061	.064	.364	.779	1.000

**Table 32. SNK Analysis of Homogeneous Subsets at 21.1°C**

Variance	N	Subset							
		1	2	3	4	5	6	7	8
8.00	3	11432.3333							
16.00	3	11622.0000							
12.00	3	15120.0000	15120.0000						
7.00	3	23238.6667	23238.6667						
4.00	3	23823.0000	23823.0000						
15.00	3	24666.6667	24666.6667						
11.00	3		27911.0000	27911.0000					
14.00	3			36379.6667	36379.6667				
3.00	3				40570.0000	40570.0000			
6.00	3				42200.0000	42200.0000			
13.00	3				44761.3333	44761.3333			
10.00	3					51203.0000	51203.0000		
5.00	3						59236.6667		
2.00	3							68957.3333	
9.00	3							70366.3333	
1.00	3								91593.6667
Sig.		.061	.055	.069	.263	.105	.083	.756	1.000

## Appendix E: MatLAB Code for $G^*$ Back Calculation

```
clear all;clc

VFA = 67.75;
VMA = 21.34;
e_star = 1199393;

G = 0:1:145000;
for i = 1:length(G)
    p(i) = (20+VFA*3*G(i)/VMA)^0.58/(650+(VFA*3*G(i)/VMA)^0.58);
    E(i) =
p(i)*(4200000*(1-VMA/100)+3*G(i)*VFA*VMA/10000)+(1-p(i))/((1-VMA/100)/42
00000+VMA/3/VFA/G(i));
end

temp = 400000;
for i = 1:length(G)
    if (abs(E(i) - e_star) <= temp)
        temp = abs(E(i) - e_star);
        out = G(i);
    end
end
out
```

## Appendix F: MatLAB Code for Reduction of Dynamic

### Modulus Results

```
% Program to reduce dynamic modulus test data file

clear all;clc;

Area = 4*pi; % Area of cross section of specimens
Lg = 70; % Gauge length, unit in mm
RAW = xlsread ('D:\Study\Research\Thesis 2\Dynamic Modulus
Results\1A_21.1.xlsx','10');
Fre = 10*2*pi;
% Data = RAW(:,1:8)
Disp_I = abs (RAW(:,2)-RAW(1,2)*ones(length(RAW(:,2)),1));
Disp_II = abs (RAW(:,4)-RAW(1,4)*ones(length(RAW(:,4)),1));
length_I = length(Disp_I);
Time = RAW(length_I-499:length_I,8);

% Calculate elements for Matrix A

a11 = 500;
a12 = sum (Time);
a13_temp = cos(Fre*Time);
a13 = sum(a13_temp);
a14_temp = sin(Fre*Time);
a14 = sum(a14_temp);
a22 = sum(Time.^2);
a23 = sum(Time.*a13_temp);
a24 = sum(Time.*a14_temp);
a33 = sum(a13_temp.^2);
a34 = sum(a13_temp.*a14_temp);
a44 = sum(a14_temp.^2);
A = [a11,a12,a13,a14;
     a12,a22,a23,a24;
     a13,a23,a33,a34;
     a14,a24,a34,a44];
```

```

% Take the last 500 point for each of the recorded data

% Displacement measured from vertical I LVDT
Disp_I = Disp_I(length_I-499:length_I);
AverageDisp_I = mean(Disp_I);
CentDisp_I = Disp_I-AverageDisp_I*ones(length(Disp_I),1);

% Displacement measured from vertical II LVDT
Disp_II = Disp_II(length_I-499:length_I);
AverageDisp_II = mean(Disp_II);
CentDisp_II = Disp_II-AverageDisp_II*ones(length(Disp_II),1);

% Load measured from force cell
Load = RAW(length_I-499:length_I,6);
AverageLoad = mean(Load);
CentLoad = Load-AverageLoad*ones(length(Load),1);

% Calculate regression parameters for displacement I
I =
[sum(CentDisp_I);sum(CentDisp_I.*Time);sum(CentDisp_I.*a13_temp);sum(Cen
tDisp_I.*a14_temp)];
para_I = A\I;
thetaI = atan(-para_I(4)/para_I(3))*180/pi; % with a unit of degree
Disp_AmpI = sqrt(para_I(3)^2+para_I(4)^2);
Disp_driftI = para_I(2)*(Time(500)-Time(1))/Disp_AmpI*100; % as percentage
Pred_Disp_I =
para_I(1)*ones(length(Disp_I),1)+para_I(2)*Time+para_I(3)*a13_temp+para_
I(4)*a14_temp;

% plot(Time,CentDisp_I,'o');
% hold on;
% plot(Time,Pred_Disp_I);

% Calculate regression parameters for displacement II
II =
[sum(CentDisp_II);sum(CentDisp_II.*Time);sum(CentDisp_II.*a13_temp);sum(
CentDisp_II.*a14_temp)];
para_II = A\II;
thetaII = atan(-para_II(4)/para_II(3))*180/pi; % with a unit of degree
Disp_AmpII = sqrt(para_II(3)^2+para_II(4)^2);
Disp_driftII = para_II(2)*(Time(500)-Time(1))/Disp_AmpII*100; % as

```

```

percentage
Pred_Disp_II =
para_II(1)*ones(length(Disp_II),1)+para_II(2)*Time+para_II(3)*a13_temp+p
ara_II(4)*a14_temp;

% figure;
% plot(Time,CentDisp_II,'o');
% hold on;
% plot(Time,Pred_Disp_II);

% Calculate regression parameters for Load
III =
[sum(CentLoad);sum(CentLoad.*Time);sum(CentLoad.*a13_temp);sum(CentLoad.
*a14_temp)];
Loadpara = A\III;
thetaLoad = atan(-Loadpara(4)/Loadpara(3))*180/pi; % with a unit of degree
Load_Amp = sqrt(Loadpara(3)^2+Loadpara(4)^2);
Load_drift = Loadpara(2)*(Time(500)-Time(1))/Load_Amp*100; % as percentage
Pred_Load =
Loadpara(1)*ones(length(Disp_I),1)+Loadpara(2)*Time+Loadpara(3)*a13_temp
+Loadpara(4)*a14_temp;

% figure;
% plot(Time,CentLoad,'o');
% hold on;
% plot(Time,Pred_Load);

% Calculate phase angle and dynamic modulus
theta_Disp = (thetaI+thetaII)/2;
% if theta_Disp <= 0.0
%     theta_Disp = theta_Disp+360;
% end
% if theta_Disp >= 180
%     theta_Disp = theta_Disp-180;
% end
%
% if thetaLoad <= 0.0
%     thetaLoad = thetaLoad-360;
% end
% if thetaLoad >= 180
%     thetaLoad = thetaLoad-180;

```

```

% end
%
% phase_angle = theta_Disp-thetaLoad
% if (phase_angle >= 90)
%     phase_angle = 180-phase_angle
% end

phase_angle = abs(abs(theta_Disp)-abs(thetaLoad))
MeanDisp_Amp = (Disp_AmpI+Disp_AmpII)/2;
DModulus = Load_Amp*(70/25.4)/MeanDisp_Amp/Area % With a unit of psi

```